Transcriptomic-Guided Optimization of Serum-Free Media for Bovine Cell Proliferation

A thesis submitted by

Ishan Ahuja

in partial fulfillment of the requirements for the degree of

Master of Science

in

Bioengineering

Tufts University

May 2024

Advisor: Dr. David Kaplan

Committee: Dr. Emmanuel Tzanakakis, Dr. Gautham Sridharan

Abstract

Fetal bovine serum (FBS)—often a critical component of animal cell culture media—is undefined, expensive, and animal-derived, opposing many of the core tenets of the cultivated meat field. Thus, serum-free media with comparable performance to existing serum-containing alternatives is a major goal. For culture of bovine satellite cells (BSC), Beefy-9 and Beefy-R are promising serum-free formulations but still underperform compared to standard growth media containing 20% FBS (BSC-GM). To improve upon their effectiveness, a transcriptomic approach was taken. From RNA sequencing of BSCs in Beefy-9, Beefy-R, and BSC-GM, differentially expressed receptors upregulated in BSC-GM were determined and those with potential proliferative effects were identified. Corresponding ligands were screened in Beefy-9 and Beefy-R; however, further optimization of Beefy-R was not achieved due to experimental difficulties. While a supplemental combination of glutamine, sphingosine-1-phosphate, and VEGF165 improved cell growth compared to Beefy-9 in short-term experiments, results were not statistically significant and proliferative effects were not observed over multiple passages. Despite no significant improvement to Beefy-9, this study provides a blueprint for future experiments to leverage similar -omics-driven optimization to narrow the gap between serum-free and serum-containing media formulations for more efficient production of cultivated meat.

Acknowledgements

I would like to first thank Dr. David Kaplan for his thoughtful guidance and support with my research and more throughout my additional year at Tufts. I would also like to thank all the members of the cellular agriculture group who I had the opportunity to learn from and who generously provided their time and advice when I had questions both in and out of the lab – thank you all for making me feel welcome! A special shout out to Benji Bromberg, whom I had the pleasure of working with on projects directly and who greatly helped with bioinformatic learning and troubleshooting. Finally, I'm incredibly grateful for the patient mentorship, advocacy, and continual support from Michael Saad—I couldn't have asked for a better role model to inspire me and help me grow as a researcher.

I'd lastly like to thank those who have supported me throughout my journey—my close friends and family. Thank you to my parents and brother for their care and constant encouragement, and to my friends for keeping me grounded and providing much-needed balance and laughs.

List of Figures

List of Tables

Chapter 1. Introduction

1.1. Cultivated Meat

Research in the field of cellular agriculture has grown tremendously over the last decade as awareness regarding problems with traditional animal agriculture systems has increased. Cultivated meat—applying tissue engineering principles to grow meat constructs from cells isolated from an animal—represents a subset of the field, which also includes fermentation-based production of proteins such as whey proteins, other food ingredients, and non-food products such as leather[1]. Concerns over animal welfare and environmental health, along with worries about potential transmission of antibiotic-resistant bacteria or zoonotic disease, have been driving factors for the field's growth[2]. Even though animal products make up only 18% of the total calories in an average global diet, the environmental impact of animal agriculture is disproportionately significant and constitutes 16–19% of total global greenhouse gas emissions[3]. While the range of emissions varies from animal to animal, animal systems as a whole contribute double the emissions of their plant-based counterparts[4,5]. Greenhouse gas emissions directly contribute to climate change, which is reflected in increasing global temperatures, severe weather events, water scarcity, and declining biodiversity[6]. Coupled with a projected 70% increase in demand for agricultural products by 2050 to satisfy a rapidly growing human population, agricultural and food industries are challenged to maintain a balance between sufficient production and environmental preservation[7].

Cultivated meat represents a possible solution, with the potential to significantly reduce greenhouse gas emissions, carbon footprint and land use in comparison to conventional beef and pork production[3,8,9]. Although life cycle analyses have predicted greater energy use than

existing animal agriculture systems[3,8,9], sustainable production of the necessary heat and electricity may be possible, a prospect less likely with existing animal feeds[3]. From animals themselves, cultivated meat would only require initial sources of cells[9], greatly improving animal welfare even compared to farming practices such as cage-free and free-range that involve less animal harm and have gained more popularity in recent years[10]. A reduction of transportation and refrigeration costs[11], increased biodiversity, and better nutritional profiles and long-term human health outcomes compared to current meat products may also be achieved[12]. Furthermore, in contrast to other alternatives to conventional meat such as plant-based or insect products, cultivated meat may come the closest in replicating textural and taste profiles, providing a perceived market advantage[11]. While personal preferences and willingness to try products will still largely dictate consumer acceptance, a clearer path forward with regards to safety has been laid, with the FDA deeming cultivated meat safe to eat in 2022[13] and the USDA approving the sale of cultivated chicken products by both GOOD Meat and UPSIDE Foods in 2023[14].

Multiple challenges including optimized culture media, bioreactor design, regulatory aspects, and consumer acceptance still remain[15]. However, $2.6 billion in funding—backing more than 150 companies—has been put into the field as of late 2022[16] with the hopes that these hurdles can be overcome and industrial production can be achieved.

1.2. Challenges with Media for Cultivated Meat

Effective and low-cost cell culture media culture media represents an important hurdle for the advancement of the cultivated meat industry, as sufficient cell growth must be balanced with a medium composition without antibiotics and animal components. With regards to the

latter, the presence of serum—largely fetal bovine serum (FBS), which is sourced from the fetus within a slaughtered pregnant cow[17]—presents the biggest challenge. While serum promotes cell proliferation and differentiation and protects cells from shear stress[15], it is mostly undefined, unsustainable, inconsistent, expensive, and animal-derived, opposing many of the core tenets of the field[18]. Furthermore, due to the conditions of the livestock beef industry, the possibility of viral, bacterial, or endotoxin contamination in serum production is present[19].

Nevertheless, serum is composed of 200–400 different proteins and thousands of metabolites such as hormones, growth factors, cytokines, and amino acids[17], making it difficult to fully replace with defined ingredients in a low-cost manner[20]. As a result, serum is typically supplemented to basal media formulations for traditional animal cell culture. However, these formulations are inherently not optimized for minimal cost, as they provide a surplus of amino acids, contain expensive buffers, and do not provide nutrient levels that cells would be exposed to *in vivo*[2]. Furthermore, since applications are largely related to biopharmaceutical production processes, their costs are significant due to strict process sterility requirements. Such formulations are viable since these costs are offset by the high value of the resulting products, namely monoclonal antibodies and cellular therapeutics. This stands in contrast to desired media formulations for cultivated meat applications, which should be low-cost due to less stringent food-grade requirements[15] and the necessity to be competitive against traditional animal agriculture products.

1.3. Existing Serum-Free Media Formulations

Serum-free media (SFM) formulations for cell expansion have been developed previously, promoting growth in T-cells[21], Chinese hamster lung cells[22], and human

mesenchymal stem cells[23]. One study found that serum-free medium composed of Neurobasal and L15 basal media supplemented with aFGF, bFGF, calcium chloride, VEGF, LIF, and vitronectin among other components was successful in promoting proliferation in rat satellite cells[24]. Another found successful proliferation of C2C12 myoblasts in both DMEM + B27 as well as AIM-V commercial SFM, with the latter resulting in almost identical doubling times and growth profiles as in serum[25]. However, most SFM still contain animal-derived ingredients, are not optimized well for muscle cell proliferation, or are too expensive compared to serum-containing alternatives[2]. Furthermore, they can contain complex, undefined ingredients or components such as synthetic steroids that may raise regulatory concerns[18].

However, promising formulations inducing growth of bovine satellite cells (BSC)—which are more relevant for cultivated meat applications—have been recently developed[18,19,26–29]. One study found that commercially available serum-free formulations such as FBM and Essential8 were able to consistently support bovine myoblast proliferation but concluded that more growth factor optimization and improved cell attachment at initial stages of growth was necessary[19]. Later work by the same group involved development of a serum- and animal-free formulation consisting of DMEM/F-12 as the basal medium and supplementation of multiple factors including L-ascorbic acid, ITS-X, FGF-2, and VEGF among others; while long-term growth validation found comparable population doublings to BSC-GM in some passages, the cumulative number of doublings in SFM still lagged behind its serum-containing analog[26]. Another study developed a formulation containing only FGF2, fetuin, BSA, and ITS in DMEM, and demonstrated better BSC growth than in DMEM/F12 + 10% FBS over multiple passages; however, proliferation was lower in comparison to their proliferative growth medium, which in

addition to 10% FBS also contained 10% horse serum and 1 mM sodium pyruvate[27]. Finally, instead of utilizing grain-derived nutrients or animal serum, one group formulated media with microalga-derived nutrients and rat liver epithelial cell-secreted factors. Bovine myoblasts successfully proliferated—likely driven by IGF-2 and other unidentified growth factors contained in the SFM—and an increase in protein production capacity was also observed[29].

Two recently developed SFM especially relevant to this project are Beefy-9 and Beefy-R; both formulations were inspired by B8, a SFM designed for human immortalized pluripotent stem cells that costs 3% as much as commercial media due to recombinant *E.coli* production of the growth factors FGF2, TGFβ1, and NRG1. In addition, B8 contains insulin, ascorbic acid-2-phosphate, transferrin, and sodium selenite, all of which are dissolved in DMEM/F12[30]. Beefy-9, the first of the two SFM developed, utilized B8 as a base to test various supplements for increased proliferation of BSCs. While multiple components were tested—IL-6, curcumin, PDGF, linoleic acid, and oleic acid—recombinant human albumin (rAlb) proved to be the main driver behind most observed growth improvements. The addition of 800 ug/ml of rAlb thus resulted in short-term growth comparable to that in 20% FBS as well as long-term growth without sacrificing myogenicity; it was also found that 1.5 ug/cm^2 VTN was necessary for successful adherence of cells to culture plates[18]. The second formulation, termed Beefy-R, improved upon Beefy-9 with regards to cost as well as growth by replacing rAlb—which was a large driver of the cost—with rapeseed protein isolate (RPI). While other oilseed protein isolates were tested, RPI was the only one that fully recovered and even exceeded Beefy-9 activity in both short- and long-term experiments. Furthermore, BSC identity and myogenicity were maintained following the switch[28].

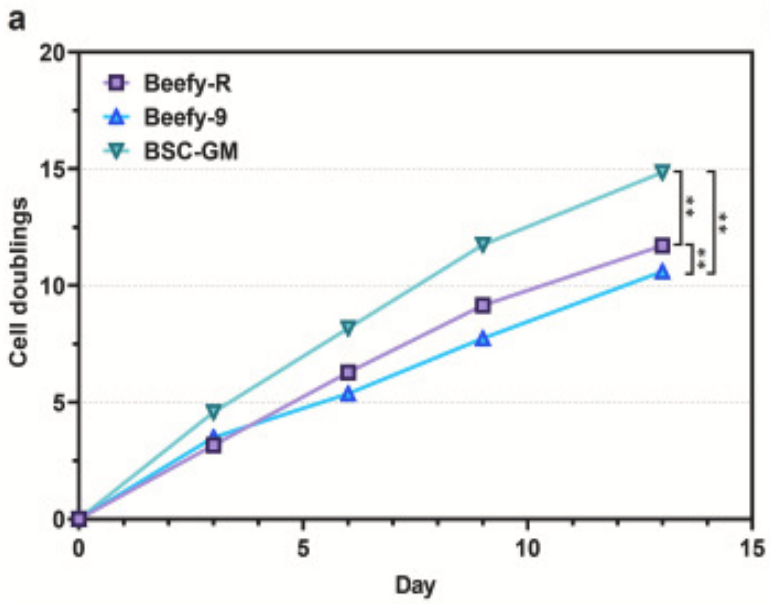

Figure 1. Cell doublings over multiple passages of BSCs cultured in BSC-GM, Beefy-9, and Beefy-R. (Stout et al., 2023).

While the formulations described above represent significant strides in the development of SFM for cultivated meat applications, further optimization in performance compared to serum-containing media is still necessary as seen in Figure 1 from Stout et al. (2023). While a further decrease in cost of media production will be required and aid in the transition to larger scales of production, it does not seem that significant technological advancements will be necessary due to the inherent difference in material costs between bench-scale—where formulations are largely developed now—and industrial scales[31].

1.4. Media Optimization Strategies

Numerous strategies have been utilized to optimize media formulations, ranging from purely experimental to mostly computational. The most traditional and straightforward is the one-factor-at-a-time (OFAT) approach, in which a single component is considered for its impact

on cell performance. However, many experiments are likely required and interaction effects are completely ignored, potentially leading to suboptimal formulations[32].

Design of experiment (DOE) techniques, which involve a series of experiments that test combinations of components as well as their interaction effects, are statistically supported, faster and more efficient at reaching optimized formulations. Designs are chosen based on experimental goals and can generally be split into classical and modern approaches with the latter being more customizable[33]. For this project, response surface designs are most relevant due to their utility primarily for optimization; specifically, they allow for the location of maxima or minima of a response with regard to a certain number of continuous factors. These designs can further be classified into central composite (an augmented factorial design with center and axial points, up to 5 levels/factor) and Box-Behnken (which allow for estimation of first- and second-order interactions but only contain 3 levels/factor) designs[34]. Other types of designs that are widely utilized include full factorial, fractional factorial, screening, mixture, split plot, and Taguchi array[33]. Drawbacks of DOE approaches include their reliance on testing of the extrema of the component concentrations and high experimental cost, especially with more than a few components[2]; as a result, their utilization is prudent for optimization of <10 variables[35]. Novel nonlinear DOE methods have been explored recently, and were found to predict optimal media component concentrations after a fewer number of experiments than a traditional DOE strategy; however, performance was limited to one passage due to the selection of the objective function, so further study will be necessary before increased adoption of this method[35].

Informatic and modeling methods such as metabolomics and metabolic flux analysis (MFA) have also been utilized for media optimization[32]. Metabolomics allows for the

quantification of metabolite levels, allowing for the determination of nutrient utilization and identification of components that could be supplemented to improve medium performance; such an approach was utilized to rationally design a media for growth of *T. brucei*[36]. More recently, a metabolomic strategy in combination with DOE was used to optimize media for chicken embryo fibroblast DF-1 cells, informing the addition of three amino acids, two vitamins, and two lipids[37]. Spent media analysis—metabolomics on spent culture media—has also been performed recently on cell types relevant to cultivated meat; however, this analysis was used to rationalize the need for cell-specific media optimization rather than optimize the media itself[38]; nevertheless, it proved to be a valuable tool for future exploration.

MFA quantifies the flux distribution in a given network and is primarily based off known stoichiometry of biological reactions and mass balances of metabolites; as a result, reaction bottlenecks as well as pathways to increase production of a specific metabolite or induce cell growth can be identified[39]. These outcomes align well with media optimization goals, thus proving useful in optimizing feed media and improving IgG antibody titer in CHO cells[40] as well as improving heterologous siderophore production via media optimization and identification of gene KO/overexpression targets in *E. coli* K-12 MG1655[41]. Although not applied to the cultivated meat field yet—largely due to the lack of experimentally-validated genome-scale metabolic models for relevant organisms— understanding species-specific metabolism can assist with accelerated and more effective media optimization for each cell type[42].

Finally, with advances in computing power and predictive capacity, more advanced computational strategies have been utilized more frequently. For example, stochastic optimization methods such as genetic algorithms[2] and Bayesian optimization tools[43] have both

been used for successful cultivated meat media optimization. A combination of an artificial neural network and a genetic algorithm has also been applied towards a reduced-serum media formulation for a zebrafish cell line, optimizing multiple objectives simultaneously important to the cultivated meat field such as yield, environmental impact, and cost[44].

1.5. RNA Sequencing

Omics techniques such as DNA sequencing, RNA sequencing (RNA seq), proteomics, and meta-and epigenomic analyses represent powerful new advances in the next-generation sequencing (NGS) toolbox. Their utilization can thus help gain a better understanding about disease states and develop insights for personalized medicine. The technology has advanced significantly over the last two decades, greatly increasing the data output and cost-effectiveness per run[45]. Here, we focus on the transcriptome specifically, which links the genomic level—which is farthest from the cellular phenotype—and the proteomic level, which quantifies proteins to determine biological activity. The transcriptome describes the RNA profile of a cell or organism that has been transcribed from DNA, and is dynamic, reacting to physiological or pathological conditions and reflecting the current cellular or organismal state. As a result, transcriptomics serves as an effective method to characterize how external conditions such as media formulation impact cellular functions. While multiple techniques including microarrays and real-time reverse transcriptase PCR (RT-PCR) have been and can be utilized to characterize the transcriptome, RNA seq in its current form represents the “gold standard” approach, performing better in efficiency, sensitivity, precision, accuracy, and coverage than previous approaches[46]. Besides general (bulk) RNA seq that identifies and quantifies transcripts from samples that can be mixed in composition, single-cell analyses have also emerged in recent

years as potent technologies that allow for a deeper look at cellular heterogeneity in a population as well as identification of cell type and lineage[45].

In the cultivated meat field, RNA seq has been used both to characterize differences between cell lines or cell states as well as optimize media formulations. With regards to cell characterization, one study generated and analyzed gene expression data of chicken fibroblasts; namely, they compared primary and immortalized as well as adherent and suspension cell lines, showing that immortalization did not affect cell identity and cell lines clustered together regardless of breed[47]. Another group investigated the molecular changes during chicken fibroblast transdifferentiation into muscle and intramuscular fat, confirming an enrichment of myogenic- and adipogenic-specific pathways and a loss of fibroblast identity[48].

Especially pertinent to media optimization is a study that examined the transcriptomic landscape of BSCs while they were undergoing myogenic differentiation induced by serum starvation. This differentiation protocol required serum in the media for proliferation beforehand, so an alternative, serum-free strategy was desired. Using an RNA seq dataset that captured molecular changes over 96 hours of differentiation at five time-points, genes upregulated between 0–96 h were identified and found to largely encode for proteins involved in muscle development, protein folding, and cell cycle inhibition. It was then hypothesized that cell-surface receptors upregulated during the first 48 h could promote the initiation of differentiation in the absence of serum; receptors in this group were found to especially mediate signaling of insulin, transferrin, and LPA. Supplementing their corresponding ligands to basal serum-free media created a differentiation formulation that resulted in fusion indices comparable to those of the serum starvation controls. Furthermore, similar expression of

myogenic markers was supported by comparing RNA seq datasets of serum-free and serum starvation-induced differentiation from both prior to and after differentiation. It was shown that the serum-free differentiation media resulted in 3D bioartificial muscle constructs, which are necessary to validate media use towards cultivated meat applications[49]. Overall, the study demonstrated that transcriptomic-guided optimization can be successful utilized for serum-free media formulations.

1.6. Objectives

The aims of this study were two-fold for transcriptomic-guided optimization of serum-free media formulations for bovine satellite cells: (1) identify components upregulated in BSC-GM media that are instrumental in cell proliferation from transcriptomic data; and (2) optimize existing serum-free formulations (Beefy-9 and/or Beefy-R) with previously identified components utilizing a design of experiments methodology.

Chapter 2. Materials and Methods

2.1. Immortalized bovine satellite cell culture

Immortalized BSCs (iBSCs) that were previously cryopreserved in liquid nitrogen were utilized. Cells were thawed and resuspended in BSC-GM, comprised of 20% fetal bovine serum (FBS; ThermoFisher #26140079), 1 ng/mL human FGF-2 (ThermoFisher #68-8785-63), and 1% Antibiotic/Antimycotic 100X (Anti-Anti; ThermoFisher #15240062) supplemented to DMEM + Glutamax (ThermoFisher #10566024, Waltham, MA, USA). The media was 0.22 μm sterile-filtered before use. 2.5 ug/ml puromycin (ThermoFisher #A1113803) was added post-filtration to BSC-GM in order to continuously select for the engineered iBSCs. Cells were seeded at 1,500 cells/cm^2 in tissue-culture flasks and grown at 37ºC for 2–3 days until reaching 70–80% confluence. Passaging was done using a standard protocol; briefly, the media was aspirated, and the cells were washed in Dulbecco's Phosphate Buffer Solution (DPBS) (ThermoFisher #14040117). TrypLE Express (ThermoFisher #12604021) was added and cells were incubated at 37ºC for 4.5 min to facilitate cell detachment. Warmed BSC-GM (at 37ºC) was then used to neutralize the TrypLE, and cells were spun down at 300 RCF at room temperature for 5 minutes. Finally, the resulting cell pellet was resuspended in BSC-GM and counted using a NucleoCounter NC-200 to inform further seeding.

For serum-free cell culture, warmed B8 (at room temperature) was utilized instead of BSC-GM for TrypLE neutralization as well as resuspension of the cell pellet and subsequent seeding. B8 was prepared in-house by adding 200 μg/ml 2-phospho-L-ascorbic acid trisodium salt (Sigma #49752), 20 μg/ml recombinant human insulin (Sigma #91077C), 20 μg/ml recombinant human transferrin (InVitria #777TRF029), 20 ng/ml sodium selenite (Sigma

#S5261), 5.8% UltraPure H_2O (ThermoFisher #10977015), and 1% Anti-Anti to DMEM/F12 (ThermoFisher #11320033). After components were allowed to dissolve overnight at 4ºC, 0.1 ng/ml neuregulin (NRG1; PeproTech #100-03) and 0.1 ng/ml transforming growth factor (TGFβ3; R&D Systems #8420-B3-005/CF) were added. Media was stored at 4ºC as B7 until necessary for use, upon which 40 ng/ml fibroblast growth factor (FGF-2; PeproTech #100-18B) was added to make B8. In addition, 1.5 μg/cm^2 of recombinant human vitronectin (VTN; ThermoFisher #A14700) was added to B8 prior to seeding for proper cell adhesion. After at least 2 hours and at most overnight post-seeding, B8 was aspirated and replaced with either Beefy-9 or Beefy-R. Beefy-9 and Beefy-R were prepared by adding 0.8 mg/ml recombinant human albumin or 0.3 mg/ml rapeseed protein isolate to B8 respectively[28].

2.2. RNA isolation

P44 iBSCs were thawed and passaged separately in BSC-GM, Beefy-9, and Beefy-R. At P50, cells were seeded in 4 replicate T25 tissue-culture flasks per condition at 4,000 cells/cm^2 for Beefy-9 and Beefy-R and 1,500 cells/cm^2 for BSC-GM; both SFM conditions were seeded with 1.5 μg/cm^2 VTN as well. Upon reaching 80% confluence, cells were lysed with a QIAshredder (Qiagen, #79656) column and RNA was extracted using the RNeasy Mini Kit (Qiagen, #74104) according to the manufacturer's directions. Cell lysates were stored at -80ºC in ethanol. Upon thawing, RNA was subsequently purified. QC on purified RNA was performed using the nanodrop method—measuring the absorbance of a 1 uL drop of the sample—to ensure acceptable RNA quality, with ideal results being both A260/A280 and A260/A230 > 2.0[50]. Purified RNA was sent to Novogene for polyA enrichment and library preparation. RNA was sequenced on a NovaSeq 6000 (Illumina) with paired-end, 150 base-pair (bp) reads. At least 6G

per sample and GNU zipped (gz) FASTQ files were provided. Reads containing the adapter or those with low quality were filtered out before data release.

2.3. Transcriptomic data analysis

Transcript counts were quantified using Salmon v1.10.1; briefly, a gentrome was generated by concatenating the *Bos taurus* genome to the end of the transcriptome (ARS-UCD2.0). A decoy file containing the chromosome names was also generated. The salmon index was then created using the gentrome, decoy file, and a minimum k-mer size of 31[51]. Salmon was subsequently run with both paired-end FASTQ files for each of the 12 samples sequenced with 24 threads and accounting for both sequencing and GC biases. Output files were used for differential expression analysis by DESeq2[52] in R. A count matrix with gene counts from all samples was created, and clustering via principal component analysis (PCA) and heatmap correlations were performed to ensure that differences between media conditions were observed. Counts were shrunk by the ashr algorithm to reduce gene-wise dispersion[52–54]. Differential expression between serum-containing and serum-free conditions as well as between each combination of the three conditions was performed in R. A negative binomial Wald test with a significance cutoff of BH-FDR < 0.01 (adjusted p-value) and log2 fold change (log2FC) cutoff of 0.585 (corresponding to a fold change difference of 1) were utilized. Finally, gene set enrichment analysis[55] (GSEA) and signaling pathway impact analysis[56] (SPIA) were performed; the genome-wide annotation for bovine[57] and gene ontology (GO), KEGG, and Molecular Signatures Database (MSigDB) Hallmark gene sets were used to identify upregulated and downregulated pathways between conditions.

2.4. Ligand identification and screening

Differentially expressed genes between BSC-GM and the combined serum-free conditions were ranked using the metric $log2FC * -\log(p\ value)$ in descending order. Next, genes were filtered by searching for "receptor" contained in the full gene name; lists of top upregulated receptors (where rank > 0) and downregulated receptors (rank < 0) were generated. The same lists were generated for BSC-GM vs. Beefy-9 and BSC-GM vs. Beefy-R datasets individually in order to cross-validate top receptor targets. A literature search was then performed to identify the highest-ranked receptors with potential proliferative effects.

Screens were performed with ligands in both Beefy-9 and Beefy-R; three levels of ligand concentration—high, medium, and low—were selected based on a literature search (Supp. Table 1). P35 iBSCs (P1 in SFM) were seeded in 96-well tissue culture plates at 6,000 cells cells/cm^2. DMEM/F12 with 2.5 ug/ml puromycin was used as seeding medium and was replaced after 3 hours with ligand-supplemented media. Following 3 days of growth, media was aspirated, and the cells were rinsed with DPBS. Plates were frozen at –80ºC for 1 day. After allowing the plates to thaw for 1 hour, the CyQuant cell proliferation assay (ThermoFisher #C7026) was utilized according to the manufacturer's instructions to quantify media performance.

2.5. Short-term growth analysis

A three-component central composite design was used to create 20 unique combinations to test based off the three most effective ligands from the screen; 2 center points and an inscribed axial value of 1.667 was utilized. P72 iBSCs (P25 in SFM) were seeded in 96-well tissue culture plates at 6,000 cells cells/cm^2, again with DMEM/F12 containing 2.5 μg/ml

puromycin that was replaced after 3 hours. Following 3 days of growth, media was aspirated, and the cells were rinsed with DPBS. Hoechst 33342 nucleic acid stain (ThermoFisher #H3570) was used according to the manufacturer's instructions (diluted 1:2000 in DPBS) to quantify cell number for each of the different formulations. A Celigo imaging cytometer (Revvity #200-BFFL-5C) was then used to image and count the cells.

2.6. Multi-passage growth analysis

In order to evaluate the multi-passage proliferative effects of the top-performing formulation from the DOE, 47 iBSCs (P3 in SFM) were seeded in 6-well culture plates at 4,500 cells/cm^2, with three replicates for both the optimized Beefy-9 formulation from the DOE and Beefy-9. The DMEM/F12 media containing 2.5 μg/ml puromycin used for seeding was replaced with the optimized media and Beefy-9 respectively after 3 hours. Three replicates of P47 iBSCs in BSC-GM were also seeded at 2,000 cells/cm^2. Cells were fed after 2 days, and upon reaching 80% confluency, were passaged as described in Section 2.1 above. Each individual replicate was counted using a NucleoCounter NC-200 automated cell counter. This process was repeated over three passages. An overview of the complete experimental workflow of this study concluding with the multi-passage growth analysis described above is depicted below in Figure 2.

2.7. Statistical analysis

Statistical analysis was performed with GraphPad Prism 10.2.0 software (San Diego, CA, USA). One-way ANOVAs—both ordinary and with a Welch correction for unequal variances—with Dunnett's multiple comparisons test were performed to analyze the screens and short-term growth studies. For analysis of multi-passage growth, a two-way ANOVA was performed

with a Tukey's HSD post-hoc test between all samples for each passage. P-values < 0.05 were treated as significant. Errors are given as ± standard deviation.

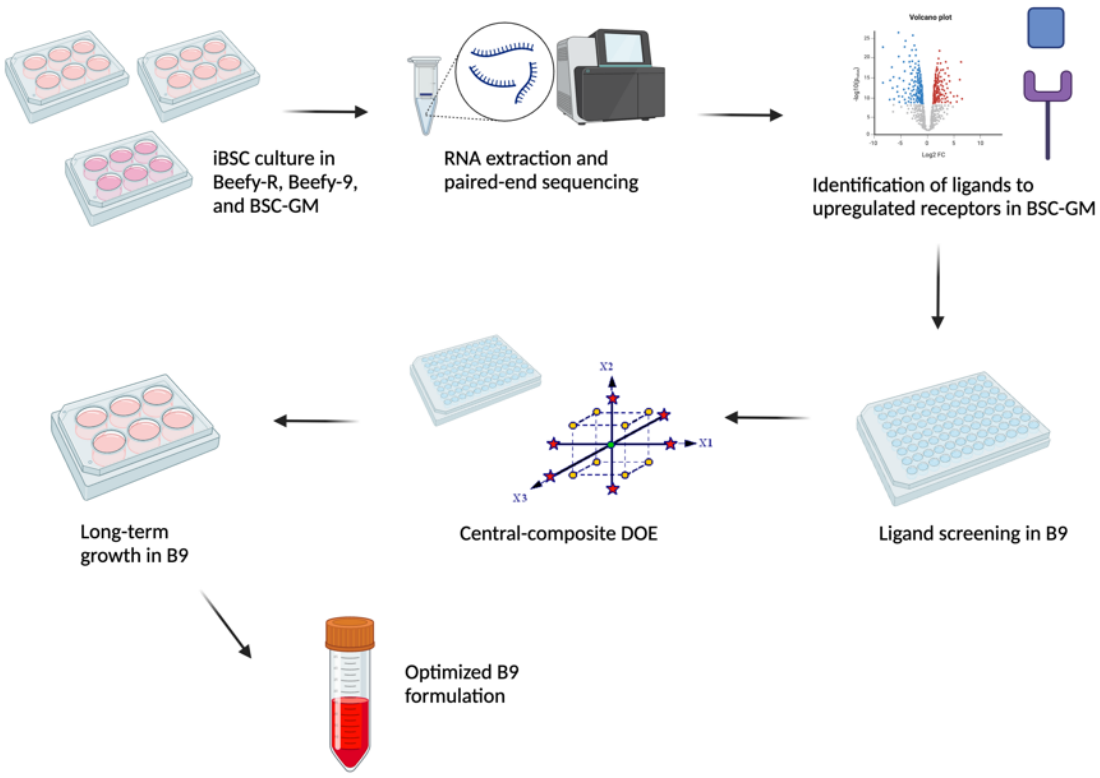

Figure 2. Overview of experimental workflow described in this study.

Chapter 3. Results

3.1. Identification of upregulated receptors in BSC-GM

RNA sequencing was performed by Novogene on four replicates of iBSCs cultured in each of BSC-GM, Beefy-9, and Beefy-R. Quality was deemed sufficient by Nanodrop (Supp. Table 1) and Novogene quality control for sequencing. Verification of replicate similarity and differences in condition was accomplished by using principal component analysis (PCA) and hierarchical clustering (Fig. 3a, b). The PCA plot confirmed that the presence of serum in the culture media was the largest contributor to sample variability, and the heatmap showed that replicates of each condition were most similar to each other, clustering together with correlation scores > 0.999. Genes were fitted to a model and counts were shrunk to reduce dispersion (Supp. Fig. 1). From differential expression analysis between BSC-GM and the two SFM conditions and using a log2FC > 0.585 and padj < 0.01, 965 out of 29,930 genes were found to be significant and upregulated in BSC-GM, while 1731 were significant and downregulated. Significant genes were different between media conditions (Fig. 3c), with Beefy-9 and Beefy-R sharing similar gene profiles. Genes were plotted on a volcano plot for visualization and the top 10 significantly upregulated receptors according to the rank metric were labeled (Fig. 3d).

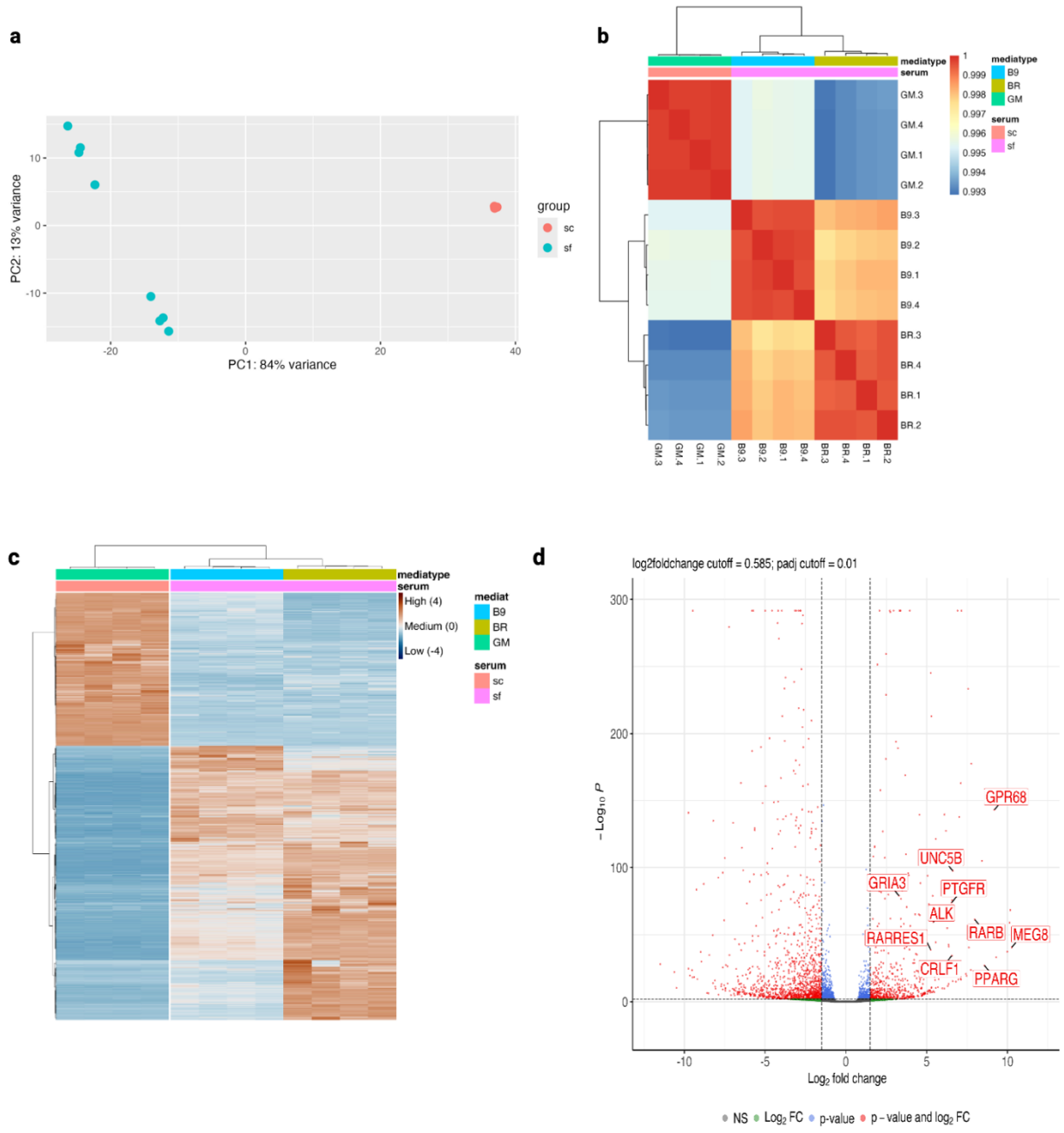

Figure 3. Quality control of samples and differential expression results. (a) Quality control using PCA to confirm differences in media condition. (b) Quality control using hierarchical clustering to confirm sample similarity. (c) Hierarchical clustering of significant genes identified by differential expression analysis. (d) Volcano plot of all differentially expressed genes with top 10 significantly upregulated receptors according to the rank metric labeled. Log2FC is defined as log2(gene expression in BSC-GM/gene expression in SFM).

Gene set enrichment analysis (GSEA) was also performed to gain additional insights into differences between BSC-GM and SFM-cultured cells. Significant pathways—with an adjusted p-value < 0.01—were identified and plotted based on their normalized enrichment score, with positive values signifying upregulation in BSC-GM and negative values downregulation; scores were normalized to a range of [-2, 2] automatically according to mean enrichment of random gene sets within the dataset of the same size[58,59]. DNA replication and cell cycle terms were notably found in both gene ontology (GO) and KEGG analyses to be upregulated in BSC-GM compared to SFM, likely reflecting the increased proliferation capability of cells in serum-containing medium (Fig. 4a, b). Additional upregulated terms such as chromosome organization, ribosome biogenesis, and G2M checkpoint also align with this hypothesis (Fig. 4a-c). Specific signaling pathways implicated in growth—namely PI3K-Akt, TGF-beta, and calcium signaling in addition to others—were upregulated in BSC-GM (Fig. 4d). Expression distributions based on fold change of most significant GO and KEGG gene pathways were also visualized (Supp. Fig. 2).

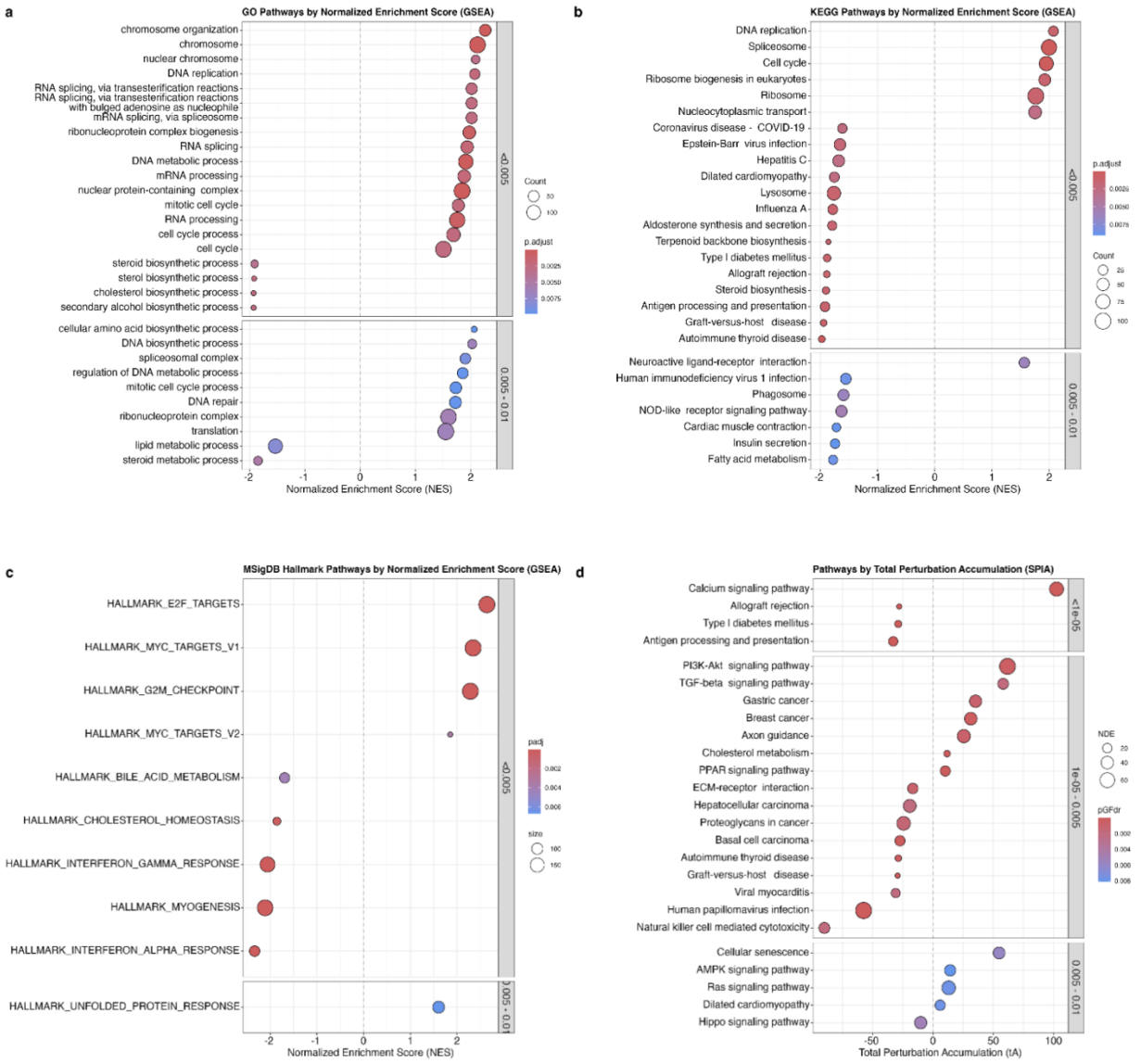

Figure 4. Pathway enrichment analysis of differentially expressed genes. (a) GSEA performed with GO terms. (b) GSEA performed with KEGG terms. (c) GSEA performed with MSigDB Hallmark gene set. (d) Pathways with greatest total perturbation accumulation from SPIA analysis.

Following ranking of the significant upregulated differentially expressed genes and filtering for receptors, a literature search was performed on the receptors with a rank metric > 100 (Table S2) to identify associated ligands with potential proliferative effects. 10 ligands corresponding to 10 of the identified receptors were identified and selected for further

screening (Table 1). Two additional ligands—PGE2 and LPA—were not identified from the transcriptomic analysis but were available in the lab and similar to other tested ligands, namely PGF2α and S1P respectively; both ligands also have been shown to induce cell proliferation (Table 1). In addition, both bind to G-protein coupled receptors, many of which—including the receptors for PGF2 and PGD2—were identified as significant and upregulated in the performed analysis.

Receptor	**Ligand**
Unc-5 netrin receptor B (UNC5B)	Netrin-1[60–62]
DCC netrin 1 receptor (DCC)	
Prostaglandin F receptor (PTGFR)	Prostaglandin F2 alpha (PGF2α)[63–65]
ALK receptor tyrosine kinase (ALK)	Pleiotrophin (PTN)[66,67]
	Heparin[68,69]
Notch receptor 1 (Notch-1)	Delta-like ligand 4 (DLL4)[70,71]
Kinase insert domain receptor KDR (RTK)	Vascular endothelial growth factor (VEGFa/VEGF165)[26,72–74]
G protein-coupled receptor 63 (GPR63)	Sphingosine-1-phosphate (S1P)[75–77]
Retinoic acid receptor beta (RAR)	Retinoic acid (RA)[78–81]
Angiotensin II receptor type 1 (AGTR1)	Angiotensin II (ATII)[82–85]
Glutamate ionotropic receptor AMPA type subunit 3 (GRIA3)	Glutamine (Gln)[86,87]
N/A	Prostaglandin E2 (PGE2)[88,89]
	Lysophosphatidic acid (LPA)[90,91]

Table 1. Receptors and associated ligands selected for screening to improve SFM. Sources indicating potential to induce proliferation are cited.

3.2. Ligand screening

The identified ligands were screened as supplements to Beefy-9 and Beefy-R to determine respective effects on short-term (3 day) growth of iBSCs. The first screen performed

included both Beefy-9 and Beefy-R but resulted in low CyQuant values across all conditions (Fig. 5a, b); in combination with the fact that there was large variability between replicates, it was determined that the best path forward would be to redo the experiment. Utilizing this data as a rough approximation however, three of the worst-performing ligands—netrin-1, PGF2α, and retinoic acid—were eliminated for ease of future experiments. Unfortunately, even seeding with a sufficient number of iBSCs was not able to be achieved for Beefy-R screening experiments over multiple attempts; as a result, ligands were only further screened in Beefy-9 for optimization. A successful Beefy-9 screen (n = 3) resulted in sufficient CyQuant fluorescence values to draw accurate results from; both an ordinary one-way analysis of variance (ANOVA) and a Welch ANOVA test were performed to capture differences in mean with both equal and unequal variances between ligand conditions respectively (Fig. 5c, d). In addition, Dunnett's multiple comparisons test was performed to compare the control Beefy-9 with each individual experimental condition. From this test, it was observed that formulations with each of 0.125 mM glutamine, 10 ng/ml VEGF165, and 100 ng/ml S1P resulted in statistically significant increased growth relative to Beefy-9. As a result, these three components were taken forward for a DOE optimization approach.

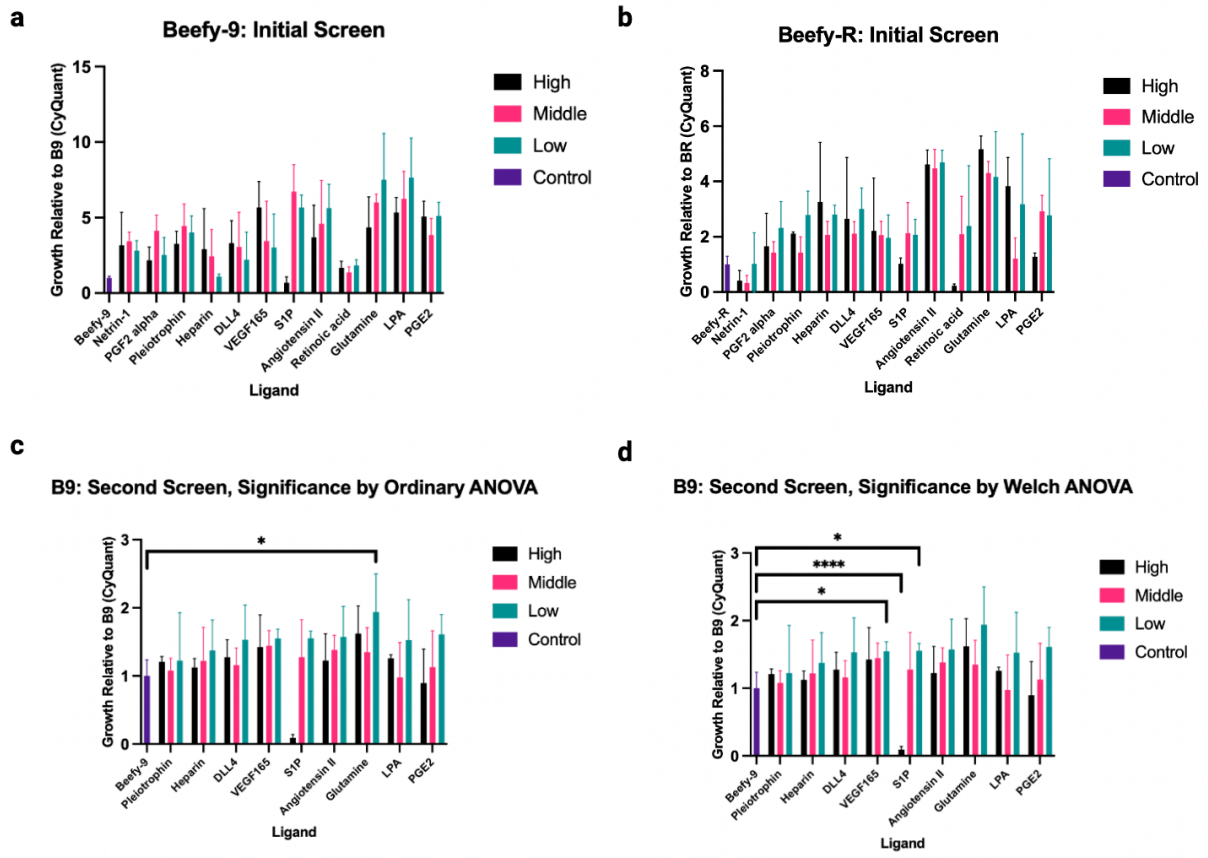

Figure 4. Results from screening experiments in Beefy-9 and Beefy-R. n = 3 distinct samples for all screens. (a) Initial three-day screen in Beefy-9 with complete set of ligands. (b) Initial three-day screen in Beefy-R. (c) Second screen in Beefy-9 with reduced set of ligands determined from initial screen. Statistical significance was calculated by an ordinary one-way ANOVA with Dunnett's multiple comparisons test and is indicated with $p < 0.05$ (*). (d) Second screen in Beefy-9 with reduced set of ligands. Statistical significance calculated by Brown-Forsythe and Welch ANOVA with Dunnett's multiple comparisons test, assuming unequal variances; significance indicated with $p < 0.05$ (*) and $p < 0.001$ (****).

3.3. Short-term growth analysis with DOE

Following a successful screening experiment in Beefy-9, a central composite design was utilized to further elucidate effects of glutamine, S1P, and VEGF165 on cell proliferation; this design was chosen due to its ability to test multiple factor levels per ligand in a relatively controlled range around the best-performing screening concentrations. 20 formulations were

tested in replicate over a period of 3 days, with the three screening formulations containing just the individual ligands being added to 16 DOE-generated combinations and one control (Fig. 6a).

a

Condition	Pattern	Glutamine (mM)	VEGF165 (ng/ml)	S1P (ng/ml)
A	−−−	0.05	4	40
B	−−+	0.05	4	160
C	−+−	0.05	16	40
D	−++	0.05	16	160
E	+−−	0.2	4	40
F	+−+	0.2	4	160
G	++−	0.2	16	40
H	+++	0.2	16	160
I	a00	0	10	100
J	A00	0.25	10	100
K	0a0	0.125	0	100
L	0A0	0.125	20	100
M	00a	0.125	10	0
N	00A	0.125	10	200
O	000	0.125	10	100
P	000	0.125	10	100
Q	N/A	0.125	0	0
R	N/A	0	10	0
S	N/A	0	0	100
Control	N/A	0	0	0

b

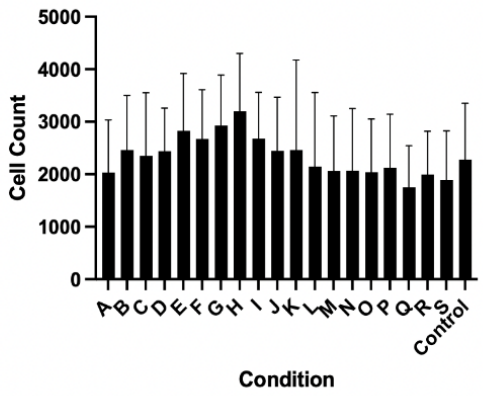

c

Comparison	p-value	Mean Difference
H vs. Control	0.1757	915.7
E vs. Control	0.4036	544.7
G vs. Control	0.2966	647

d

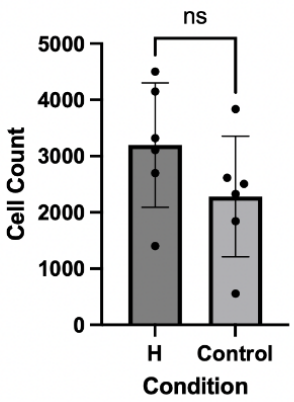

Figure 5. Results from short-term DOE in Beefy-9. (a) Three-component central composite design with inscribed axial value of 1.667. (b) Cell counts following three-day culture in corresponding media conditions. n = 6 distinct samples; no statistically significant differences were observed through calculation by an ordinary one-way ANOVA or a Brown-Forsythe and Welch ANOVA, both with Dunnett's multiple comparisons test. (c) Comparison of top three performing formulations with mean difference from control and p-value. n = 6 distinct samples; p-values were calculated from an individual Welch's t-test. (d) Comparison of condition H (0.2 mM Gln, 16 ng/ml VEGF, 160 ng/ml S1P) to control with overlayed data points; n = 6 distinct samples. No statistical significance was observed as calculated for Fig. 6b.

Although multiple experimental difficulties were faced due to uneven seeding or lack of enough iBSCs for accurate CyQuant quantification, a valid experiment was eventually performed (n = 6). Instead of CyQuant however, live-cell DAPI imaged on the Celigo was utilized to quantify

cell proliferation in an effort to reduce variability in measurement. While none of the combinations from this experiment proved to be statistically significant by either the ordinary or Welch ANOVA tests with Dunnett's multiple comparisons (Fig. 6b), three formulations resulted in considerably higher mean cell counts. Performing Welch t-tests with between these formulations and the Beefy-9 control identified that condition H was the most significant supplement combination (Fig. 6c). This formulation also resulted in consistently higher cell counts across replicates and a mean across replicates of 3196 cells compared to 2281 cells in control Beefy-9 (Fig. 6d). This media consisted of Beefy-9 supplemented with 0.2 mM glutamine, 16 ng/ml VEGF165, and 160 ng/ml S1P. Despite the lack of statistical significance, this formulation was selected to test in multi-passage growth due to time constraints and its clear performance advantages over other tested combinations.

3.4. Multi-passage growth analysis

Formulation H was utilized for a multi-passage growth analysis, which included 3 passages over a period of 10 days in 6-well culture plates. Morphology of BSCs were comparable between Beefy-9 and supplemented Beefy-9, but both are observably different than BSCs cultured in BSC-GM; microscopy images were taken on Day 2 of the third passage (Fig. 7a). While the supplemented Beefy-9 media showed an increase in growth compared to control over the first passage—similar to the short-term experiment—the second and third passages did not exhibit this same trend and the supplemented Beefy-9 was outperformed by the control with regards to cumulative cell doublings. This difference was only statistically significant following the third passage (Fig. 7b). The lower doubling time of the supplemented Beefy-9 formulation over the first passage was statistically significant in addition to the

following performance shift over the second passage; while one replicate had a clearly higher doubling time than the other two, this was determined to not be an outlier and left in the analysis. BSCs cultured in supplemented Beefy-9 recovered slightly with regards to doubling time over the third passage—no significant difference was observed between the supplemented and control media—but the experiment was stopped upon basis of the cumulative cell doubling results.

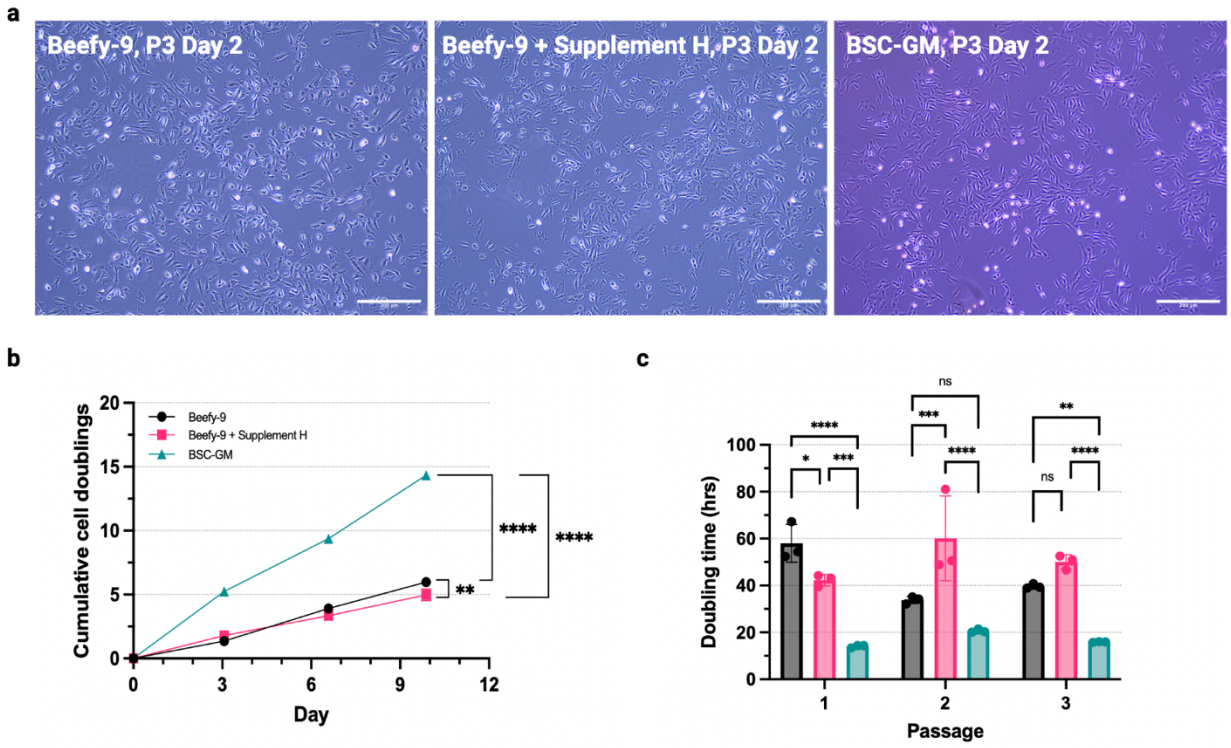

Figure 6. Multi-passage growth of iBSCs in Beefy-9 + supplement H compared to Beefy-9 control and BSC-GM. (a) Brightfield images of BSCs in day 2 of growth during the third passage of the experiment; supplemented and control Beefy-9 morphology was almost identical, but both were different than BSCs in BSC-GM. Scale bars are 200 µm. (b) Multi-passage growth over 10 days in supplemented and control Beefy-9 and BSC-GM. n = 3 distinct samples; statistical significance was calculated by two-way ANOVA and is indicated for the final timepoint with $p < 0.01$ (**) and $p < 0.001$ (****). (c) Doubling time calculated per passage for each of the three conditions in (b). n = 3 distinct samples; statistical significance was calculated by two-way ANOVA and is indicated with $p < 0.05$ (*), $p < 0.01$ (**), $p < 0.005$ (***), and $p < 0.001$ (****).

Chapter 4. Discussion

Effective serum-free media for muscle cell proliferation is necessary for the advancement of cultivated meat research, as focus in the field shifts towards adequate scale-up to reach a wider consumer base and come closer to achieving cost parity with conventional meat production. Cultivated cattle production is of particular focus, as conventional beef farming is the largest contributor to greenhouse gas emissions and land use compared to other livestock such as pork and chicken[11]. Although formulations such as Beefy-9 and Beefy-R have been developed and successful in promoting a certain degree of iBSC growth, they still lag significantly behind serum-containing BSC-GM in multi-passage culture. In this study, a transcriptomics-guided approach was utilized to attempt to further optimize iBSC SFM; specifically, ligands of receptors upregulated in cells cultured in BSC-GM were supplemented to Beefy-9, and short-term and multi-passage growth were analyzed to determine the efficacy of the supplemented Beefy-9 formulation.

From the RNA seq analysis, we observed that gene profiles differed significantly between cells cultured in serum-containing BSC-GM and SFM Beefy-9 and Beefy-R; upregulated gene sets largely pointed to increased cell growth, with many GO terms relating to various nucleic acid replication and processing activities in the cell cycle. This result was expected, given that the major observable difference between BSC-GM and SFM and the one of most interest in this study is the resulting rate of cell growth. Upregulated KEGG and MSigDB terms and gene sets also aligned closely with this result; notably, the 4 upregulated gene sets identified within the MSigDB hallmark database—E2F targets, MYC targets v1, G2M checkpoint, and MYC targets v2—represent 4 out of 6 defined by the MSigDB to be cell proliferation-related, with the other

two being mitotic spindle and p53 pathway sets. Furthermore, E2F targets and G2M checkpoint genes are strongly correlated to each other[92], which aligns with the large positive enrichment scores and high statistical significance observed in this study. Signaling pathways associated with proliferation were also identified through SPIA, with those of note including the PI3K-Akt and TGF-β pathway. TGF-β is one of the main ingredients in B8[30] (and subsequently Beefy-9 and Beefy-R as well), and induces the expression of various growth-promoting factors in smooth muscle cells and some fibroblasts at low concentrations[93]. The PI3K-Akt pathway—which also involves mTOR—mediates cell survival, migration and proliferation, and has been shown to be activated by KDR, one of the receptors targeted in this study[94]. In this experiment however, although both KDR (identified as RTK in Supp. Fig. 3) and AKT were activated, PI3K class 1A—which is contained in the pathway—was surprisingly downregulated; thus, activation of AKT may not have necessarily been via KDR, but rather through PI3K class 1B, which is shown to be upregulated (Supp. Fig. 3). Effects of the KDR receptor may instead be propagated through the MAPK/ERK pathway, which also has been shown to generally promote cell proliferation[95]. is more difficult to interpret the downregulated terms, with many of the pathways identified associated with specific diseases and not necessarily relevant to cell proliferation or even differentiation; however, it is interesting to note that some terms related to lipid and fatty acid metabolism were downregulated in both GO and KEGG analyses. In contrast, lipids have been observed by microscopy within cells cultured in SFM. Further analysis into the specific genes contained within these pathways would help to better understand their prevalence in SFM-cultured cells in contrast to BSC-GM.

Although all of the ligands selected have been shown to induce proliferation to some degree, the performances of glutamine, VEGF, and S1P align based on activation of similar pathways. Glutamine has been shown to promote proliferation through activation of the mTOR/S6 and MAPK/ERK pathways, of which the former is closely associated with the PI3K-Akt pathway found to be upregulated in BSC-GM. The latter has also been shown to influence proliferation, with downregulation resulting in decreased proliferation in multiple cases[96]. In this study, glutamine was selected over glutamate—even though glutamate is the specific ligand for GRIA3, which was identified from RNA seq—due to these alternative modes of encouraging proliferation, given the fact that glutamine naturally metabolizes to glutamate within the cell. Furthermore, glutamine is already commonly provided as a media supplement in basal media in the form of GlutaMax, which is a dipeptide that is less sensitive to pH and less likely to degrade[97]. It was interesting though that only the lowest concentration of glutamine resulted in statistically significant increased growth, but high concentration was better than an intermediate one; replacing it with either GlutaMax—which has shown to be more stable, leading to increased performance[97]—or glutamate could be helpful to explore. VEGF has also been found to induce proliferation through both the PI3K-Akt[98] and ERK[72] pathways depending on whether VEGFR-1 or VEGFR-2 are targeted; in this experiment, the latter is likely due to the identification of KDR (equivalent to VEGFR-2) as one of the top upregulated receptors. S1P can also activate ERK[75,99]; it is unsure whether the mechanism of action in this study occurred through this pathway though or if the corresponding receptor—GPR63—is involved in another pathway.

With regards to short-term proliferation, the fact that supplement H proved to be the most optimal makes sense since it contains all three ligands that proved to be statistically significant individually. In addition, the concentrations of all three were slightly above the concentration levels identified in the screen as best-performing, but still significantly lower than the middle concentration level—which resulted in worse performance for all three ligands—due to the dilution factor of 4. Unfortunately, an improvement in BSC growth not observed in multi-passage growth. While the shift in performance was surprising between the first and second passages, it should be noted that there was a replicate with a markedly increased doubling time compared to the other two for the supplemented Beefy-9 condition; although this was not statistically found to be an outlier, the statistical significance of the calculated mean doubling time could have been affected. A doubling time closer to those calculated for the other two replicates may have resulted in a lack of significance in the difference between the supplemented and control Beefy-9 conditions, in accordance with what was observed in the third passage. Although the experiment was terminated after the third passage on the basis of increasingly diverging cell doublings, the recovery in doubling time between the second and third passages provides motivation for a longer-term redo of the study. It is unclear as to the reason why the supplement worsened growth performance after one passage though, and further investigation into molecular mechanisms of action would be helpful. One hypothesis is inefficient uptake of provided nutrients; it was observed in earlier screens that higher concentrations of all three metabolites provided in the supplement led to worse growth in comparison to lower concentrations. S1P in particular was especially harmful at high concentrations. Thus, buildup of nutrients or oversaturation of receptors could lead to these

effects that were observed when metabolites were supplemented in bolus at higher concentrations.

Chapter 5. Future Work

In this study, a transcriptomic-guided workflow for the optimization of SFM for iBSC cell proliferation was utilized; while increased proliferation compared to Beefy-9 in short-term growth studies was observed, the resulting formulation consisting of Beefy-9 supplemented with 0.2 mM glutamine, 16 ng/ml VEGF165, and 160 ng/ml S1P unfortunately did not result in an improvement over Beefy-9 in multi-passage growth. As a result, multiple next steps can be considered.

First, experiments performed in this study can be repeated for greater accuracy; even though statistically significant supplements were identified through ligand screening, error bars were still relatively large across experiments regardless of quantification method. For future studies, live-cell DAPI should likely be utilized due to advantages in clarity of results—direct quantification of cell number, in comparison to fluorescence capturing the DNA content of the whole sample[100]—as well as lower cost. An increased number of replicates for screening and more even cell seeding could be objectives in order to obtain more reliable results. For the latter, letting cells incubate at room temperature following seeding has been shown to significantly reduce cell clustering in edges of wells[101], a problem that was present in multiple experimental runs in this study. While this technique was adopted for short-term and multi-passage experiments, plates were only incubated for 15–30 min at RT in contrast to one hour suggested by the paper; using a longer incubation time could lead to more consistent seeding. For multi-passage experiments, although results were more consistent across replicates than for screening or short-term experiments, some replicates were quite different from others without

being classified statistically as outliers; thus, repeating this experiment with more replicates may also lead to more consistent and significant results.

Running the same experimental workflow with Beefy-R would also be a logical next step, given that the receptors identified from the transcriptomic analysis was based on a combination of genes in both SFM formulations. While testing supplement H in Beefy-R could be worth a try, the results from the initial screening of ligands—albeit with low CyQuant values—suggest that different ligands have different effects between Beefy-R and Beefy-9; as a result, starting from scratch would likely result in a more optimized formulation. In fact, using individualized differential expression analysis between Beefy-9/Beefy-R alone and BSC-GM allows for identification of upregulated receptors specific to that medium only and would likely lead to better results for optimization of both SFM.

Experiments to confirm the activation of the targeted receptors—via qPCR or a similar analytical method—would help to determine whether the short-term growth increase and long-term inhibitory effects of the supplement were due to the expected activation of the glutamine, VEGF, and S1P receptors or additional mechanisms of action. Comparing to a control with just SFM would allow for the determination of up- or downregulation of these receptors. Looking at alternative receptors that could be activated by glutamine, VEGF165, and S1P could also help to elucidate the reasons behind the growth patterns that were observed upon supplementation. Furthermore, additional experiments testing the supplement with components removed from the SFM basal media—such as insulin, FGF2, or TGF$\beta 3$—would be interesting to explore, as these components may share similar activation pathways and could thus potentially be competing or oversaturating receptors; as a result, the potential growth effects imbued by the

supplement could either be masked or even negated by the effects of these growth factors already present in the media. Testing the supplement in a B8 basal media instead of a Beefy-9 or Beefy-R base could also help inform if competing effects are observed due to either albumin or RPI respectively. Finally, looking deeper into the terms identified as upregulated with pathway enrichment analysis (GO, KEGG, MSigDB, and SPIA) would be a helpful area of future exploration; since many of these gene sets were associated with cell replication or cell cycle—likely corresponding to the increased proliferation observed in BSC-GM—it would be helpful to confirm if the receptors identified in this study belonged to those gene sets. In addition, the other genes contained in these gene sets could also be investigated further for their potential ability to induce increased proliferation; if these genes are able to be modulated easily, experiments could then be performed to further test these hypotheses.

Pairing the transcriptomic analysis with additional -omics datasets could result in more effective optimization. For example, proteomics was utilized by Stout et al. (2023) to characterize differences in oilseed protein isolates that improved iBSC growth in B8 and identify potential proteins contributing to the efficacy of specific isolates. Furthermore, it can be a useful complementary technique to RNA seq to validate the presence of protein products predicted by mRNA transcripts since regulation of translation may result in differing protein expression. Post-translational modifications—some of which can be detected with proteomic techniques—are also especially important with regards to protein activity but cannot be detected on the transcript level. Finally, since proteins are the effectors of physiological change in the cell, monitoring these as closely as possible can allow for a greater understanding of cellular processes. Proteomics has already been performed for iBSCs cultured in Beefy-9, Beefy-

R, and BSC-GM, and experiments are underway following the identification of significantly expressed proteins between BSC-GM and the SFM; combining effective supplements found using proteomics with the results from this study could thus lead to a more optimized SFM formulation.

Originally in the scope of this study, a metabolomics approach using spent media analysis is a potential area of exploration. Spent media analysis (SMA) allows for the understanding of the utilization of various nutrients present in media[38]. Recently, the technique has been applied to cultivated meat cell lines—namely primary embryonic chicken muscle cells and fibroblasts as well as murine C2C12 myoblast cells—to determine if there were significant species- or cell-type differences in nutrient utilization. It was found that utilization of glucose, glutamine, FGF2, and other amino acids, growth factors, and vitamins differed between the three cell types, implying inherent metabolic differences between cell types. Furthermore, many nutrients were not noticeably depleted, suggesting they may not be necessary in formulations for cultivated meat[38]. Results from SMA would most directly lead to identification of metabolites either present at greater quantities at BSC-GM or depleted quicker in SFM that can be supplemented. Combining metabolite levels with genome-scale annotation and experimental pathway information could also lead to the generation of a genome-scale metabolic model (GEM), which are largely lacking for cultivated meat-relevant cell types[102] but are critical to performing metabolic flux analysis (MFA) in order to quantify the flux distribution in a given network. MFA could help identify reaction bottlenecks as well as pathways to induce cell growth[39] guiding further media optimization or even genetic engineering of cell lines, which has already been utilized to eliminate FGF2 growth factor requirements in engineered bovine

cells[103] and could work alongside media development for optimized cell growth or differentiation.

Finally, the consideration of both cost and environmental life cycle analysis of any SFM developed or optimized further in the future is necessary. Neither of these factors were considered in this study, but they will be increasingly important to look at in order to determine feasibility at larger, industrial scales that will eventually be necessary.

Chapter 6. References

(1) Stephens, N.; Di Silvio, L.; Dunsford, I.; Ellis, M.; Glencross, A.; Sexton, A. Bringing Cultured Meat to Market: Technical, Socio-Political, and Regulatory Challenges in Cellular Agriculture. *Trends in Food Science & Technology* **2018**, *78*, 155–166. https://doi.org/10.1016/j.tifs.2018.04.010.

(2) O'Neill, E. N.; Cosenza, Z. A.; Baar, K.; Block, D. E. Considerations for the Development of Cost-Effective Cell Culture Media for Cultivated Meat Production. *Comprehensive Reviews in Food Science and Food Safety* **2021**, *20* (1), 686–709. https://doi.org/10.1111/1541-4337.12678.

(3) Sinke, P.; Swartz, E.; Sanctorum, H.; van der Giesen, C.; Odegard, I. Ex-Ante Life Cycle Assessment of Commercial-Scale Cultivated Meat Production in 2030. *Int J Life Cycle Assess* **2023**, *28* (3), 234–254. https://doi.org/10.1007/s11367-022-02128-8.

(4) Lynch, J.; Pierrehumbert, R. Climate Impacts of Cultured Meat and Beef Cattle. *Frontiers in Sustainable Food Systems* **2019**, *3*.

(5) Xu, X.; Sharma, P.; Shu, S.; Lin, T.-S.; Ciais, P.; Tubiello, F. N.; Smith, P.; Campbell, N.; Jain, A. K. Global Greenhouse Gas Emissions from Animal-Based Foods Are Twice Those of Plant-Based Foods. *Nat Food* **2021**, *2* (9), 724–732. https://doi.org/10.1038/s43016-021-00358-x.

(6) Nations, U. *What Is Climate Change?*. United Nations. https://www.un.org/en/climatechange/what-is-climate-change (accessed 2023-12-21).

(7) Rojas-Downing, M. M.; Nejadhashemi, A. P.; Harrigan, T.; Woznicki, S. A. Climate Change and Livestock: Impacts, Adaptation, and Mitigation. *Climate Risk Management* **2017**, *16*, 145–163. https://doi.org/10.1016/j.crm.2017.02.001.

(8) Tuomisto, H. L.; Allan, S. J.; Ellis, M. J. Prospective Life Cycle Assessment of a Bioprocess Design for Cultured Meat Production in Hollow Fiber Bioreactors. *Science of The Total Environment* **2022**, *851*, 158051. https://doi.org/10.1016/j.scitotenv.2022.158051.

(9) Rubio, N. R.; Xiang, N.; Kaplan, D. L. Plant-Based and Cell-Based Approaches to Meat Production. *Nat Commun* **2020**, *11* (1), 6276. https://doi.org/10.1038/s41467-020-20061-y.

(10) Schaefer, G. O.; Savulescu, J. The Ethics of Producing In Vitro Meat. *Journal of Applied Philosophy* **2014**, *31* (2), 188–202. https://doi.org/10.1111/japp.12056.

(11) Treich, N. Cultured Meat: Promises and Challenges. *Environ Resource Econ* **2021**, *79* (1), 33–61. https://doi.org/10.1007/s10640-021-00551-3.

(12) Luiz Morais-da-Silva, R.; Glufke Reis, G.; Sanctorum, H.; Forte Maiolino Molento, C. The Social Impacts of a Transition from Conventional to Cultivated and Plant-Based Meats: Evidence from Brazil. *Food Policy* **2022**, *111*, 102337. https://doi.org/10.1016/j.foodpol.2022.102337.

(13) Gibson, K. *FDA approves lab-grown meat for the first time - CBS News*. https://www.cbsnews.com/news/lab-grown-meat-approved-by-fda-cultivated-chicken-upside-foods/ (accessed 2024-02-21).

(14) Thompson, J. *Lab-Grown Meat Approved for Sale: What You Need to Know*. Scientific American. https://www.scientificamerican.com/article/lab-grown-meat-approved-for-sale-what-you-need-to-know/ (accessed 2024-02-21).

(15) Eibl, R.; Senn, Y.; Gubser, G.; Jossen, V.; van den Bos, C.; Eibl, D. Cellular Agriculture: Opportunities and Challenges. *Annual Review of Food Science and Technology* **2021**, *12* (1), 51–73. https://doi.org/10.1146/annurev-food-063020-123940.
(16) *The science of cultivated meat | GFI*. https://gfi.org/science/the-science-of-cultivated-meat/ (accessed 2024-02-17).
(17) Lee, D. Y.; Lee, S. Y.; Yun, S. H.; Jeong, J. W.; Kim, J. H.; Kim, H. W.; Choi, J. S.; Kim, G.-D.; Joo, S. T.; Choi, I.; Hur, S. J. Review of the Current Research on Fetal Bovine Serum and the Development of Cultured Meat. *Food Sci Anim Resour* **2022**, *42* (5), 775–799. https://doi.org/10.5851/kosfa.2022.e46.
(18) Stout, A. J.; Mirliani, A. B.; Rittenberg, M. L.; Shub, M.; White, E. C.; Yuen, J. S. K.; Kaplan, D. L. Simple and Effective Serum-Free Medium for Sustained Expansion of Bovine Satellite Cells for Cell Cultured Meat. *Commun Biol* **2022**, *5* (1), 1–13. https://doi.org/10.1038/s42003-022-03423-8.
(19) Kolkmann, A. M.; Post, M. J.; Rutjens, M. A. M.; van Essen, A. L. M.; Moutsatsou, P. Serum-Free Media for the Growth of Primary Bovine Myoblasts. *Cytotechnology* **2020**, *72* (1), 111–120. https://doi.org/10.1007/s10616-019-00361-y.
(20) Post, M. J.; Levenberg, S.; Kaplan, D. L.; Genovese, N.; Fu, J.; Bryant, C. J.; Negowetti, N.; Verzijden, K.; Moutsatsou, P. Scientific, Sustainability and Regulatory Challenges of Cultured Meat. *Nat Food* **2020**, *1* (7), 403–415. https://doi.org/10.1038/s43016-020-0112-z.
(21) Eberhardt, F.; Hückelhoven-Krauss, A.; Kunz, A.; Jiang, G.; Sauer, T.; Reichman, A.; Neuber, B.; Böpple, K.; Schmitt, A.; Müller-Tidow, C.; Schmitt, M.; Keib, A. Impact of Serum-Free Media on the Expansion and Functionality of CD19.CAR T-Cells. *Int J Mol Med* **2023**, *52* (1), 58. https://doi.org/10.3892/ijmm.2023.5261.
(22) Yamano-Adachi, N.; Arishima, R.; Puriwat, S.; Omasa, T. Establishment of Fast-Growing Serum-Free Immortalised Cells from Chinese Hamster Lung Tissues for Biopharmaceutical Production. *Sci Rep* **2020**, *10* (1), 17612. https://doi.org/10.1038/s41598-020-74735-0.
(23) Chase, L. G.; Lakshmipathy, U.; Solchaga, L. A.; Rao, M. S.; Vemuri, M. C. A Novel Serum-Free Medium for the Expansion of Human Mesenchymal Stem Cells. *Stem Cell Research & Therapy* **2010**, *1* (1), 8. https://doi.org/10.1186/scrt8.
(24) McAleer, C. W.; Rumsey, J. W.; Stancescu, M.; Hickman, J. J. Functional Myotube Formation from Adult Rat Satellite Cells in a Defined Serum-Free System. *Biotechnol Prog* **2015**, *31* (4), 997–1003. https://doi.org/10.1002/btpr.2063.
(25) Jang, M.; Scheffold, J.; Røst, L. M.; Cheon, H.; Bruheim, P. Serum-Free Cultures of C2C12 Cells Show Different Muscle Phenotypes Which Can Be Estimated by Metabolic Profiling. *Sci Rep* **2022**, *12* (1), 827. https://doi.org/10.1038/s41598-022-04804-z.
(26) Kolkmann, A. M.; Van Essen, A.; Post, M. J.; Moutsatsou, P. Development of a Chemically Defined Medium for in Vitro Expansion of Primary Bovine Satellite Cells. *Frontiers in Bioengineering and Biotechnology* **2022**, *10*.
(27) Skrivergaard, S.; Young, J. F.; Sahebekhtiari, N.; Semper, C.; Venkatesan, M.; Savchenko, A.; Stogios, P. J.; Therkildsen, M.; Rasmussen, M. K. A Simple and Robust Serum-Free Media for the Proliferation of Muscle Cells. *Food Research International* **2023**, *172*, 113194. https://doi.org/10.1016/j.foodres.2023.113194.

(28) Stout, A. J.; Rittenberg, M. L.; Shub, M.; Saad, M. K.; Mirliani, A. B.; Dolgin, J.; Kaplan, D. L. A Beefy-R Culture Medium: Replacing Albumin with Rapeseed Protein Isolates. *Biomaterials* **2023**, *296*, 122092. https://doi.org/10.1016/j.biomaterials.2023.122092.
(29) Yamanaka, K.; Haraguchi, Y.; Takahashi, H.; Kawashima, I.; Shimizu, T. Development of Serum-Free and Grain-Derived-Nutrient-Free Medium Using Microalga-Derived Nutrients and Mammalian Cell-Secreted Growth Factors for Sustainable Cultured Meat Production. *Sci Rep* **2023**, *13*, 498. https://doi.org/10.1038/s41598-023-27629-w.
(30) Kuo, H.-H.; Gao, X.; DeKeyser, J.-M.; Fetterman, K. A.; Pinheiro, E. A.; Weddle, C. J.; Fonoudi, H.; Orman, M. V.; Romero-Tejeda, M.; Jouni, M.; Blancard, M.; Magdy, T.; Epting, C. L.; George, A. L.; Burridge, P. W. Negligible-Cost and Weekend-Free Chemically Defined Human iPSC Culture. *Stem Cell Reports* **2020**, *14* (2), 256–270. https://doi.org/10.1016/j.stemcr.2019.12.007.
(31) Specht, L. An Analysis of Culture Medium Costs and Production Volumes for Cultivated Meat.
(32) Galbraith, S. C.; Bhatia, H.; Liu, H.; Yoon, S. Media Formulation Optimization: Current and Future Opportunities. *Current Opinion in Chemical Engineering* **2018**, *22*, 42–47. https://doi.org/10.1016/j.coche.2018.08.004.
(33) *Types of Design of Experiments*. https://www.jmp.com/en_in/statistics-knowledge-portal/what-is-design-of-experiments/types-of-design-of-experiments.html (accessed 2024-03-29).
(34) *What are response surface designs, central composite designs, and Box-Behnken designs?* https://support.minitab.com/en-us/minitab/help-and-how-to/statistical-modeling/doe/supporting-topics/response-surface-designs/response-surface-central-composite-and-box-behnken-designs/ (accessed 2024-03-29).
(35) Cosenza, Z.; Block, D. E.; Baar, K. Optimization of Muscle Cell Culture Media Using Nonlinear Design of Experiments. *Biotechnology Journal* **2021**, *16* (11), 2100228. https://doi.org/10.1002/biot.202100228.
(36) Creek, D. J.; Nijagal, B.; Kim, D.-H.; Rojas, F.; Matthews, K. R.; Barrett, M. P. Metabolomics Guides Rational Development of a Simplified Cell Culture Medium for Drug Screening against Trypanosoma Brucei. *Antimicrob Agents Chemother* **2013**, *57* (6), 2768–2779. https://doi.org/10.1128/AAC.00044-13.
(37) Lin, J.; Yi, X.; Zhuang, Y. Medium Optimization Based on Comparative Metabolomic Analysis of Chicken Embryo Fibroblast DF-1 Cells. *RSC Advances* **2019**, *9* (47), 27369–27377. https://doi.org/10.1039/C9RA05128G.
(38) O'Neill, E. N.; Ansel, J. C.; Kwong, G. A.; Plastino, M. E.; Nelson, J.; Baar, K.; Block, D. E. Spent Media Analysis Suggests Cultivated Meat Media Will Require Species and Cell Type Optimization. *npj Sci Food* **2022**, *6* (1), 46. https://doi.org/10.1038/s41538-022-00157-z.
(39) Yang, S.-T.; Liu, X.; Zhang, Y. Chapter 4 - Metabolic Engineering – Applications, Methods, and Challenges. In *Bioprocessing for Value-Added Products from Renewable Resources*; Yang, S.-T., Ed.; Elsevier: Amsterdam, 2007; pp 73–118. https://doi.org/10.1016/B978-044452114-9/50005-0.
(40) Huang, Z.; Xu, J.; Yongky, A.; Morris, C. S.; Polanco, A. L.; Reily, M.; Borys, M. C.; Li, Z. J.; Yoon, S. CHO Cell Productivity Improvement by Genome-Scale Modeling and Pathway

Analysis: Application to Feed Supplements. *Biochemical Engineering Journal* **2020**, *160*, 107638. https://doi.org/10.1016/j.bej.2020.107638.
(41) Swayambhu, G.; Moscatello, N.; Atilla-Gokcumen, G. E.; Pfeifer, B. A. Flux Balance Analysis for Media Optimization and Genetic Targets to Improve Heterologous Siderophore Production. *iScience* **2020**, *23* (4), 101016. https://doi.org/10.1016/j.isci.2020.101016.
(42) *Metabolic modeling for cultivated meat - The Good Food Institute*. https://gfi.org/solutions/metabolic-modeling-for-cultivated-meat/ (accessed 2024-03-26).
(43) Cosenza, Z.; Astudillo, R.; Frazier, P. I.; Baar, K.; Block, D. E. Multi-information Source Bayesian Optimization of Culture Media for Cellular Agriculture. *Biotechnol Bioeng* **2022**, *119* (9), 2447–2458. https://doi.org/10.1002/bit.28132.
(44) Nikkhah, A.; Rohani, A.; Zarei, M.; Kulkarni, A.; Batarseh, F. A.; Blackstone, N. T.; Ovissipour, R. Toward Sustainable Culture Media: Using Artificial Intelligence to Optimize Reduced-Serum Formulations for Cultivated Meat. *Science of The Total Environment* **2023**, *894*, 164988. https://doi.org/10.1016/j.scitotenv.2023.164988.
(45) Satam, H.; Joshi, K.; Mangrolia, U.; Waghoo, S.; Zaidi, G.; Rawool, S.; Thakare, R. P.; Banday, S.; Mishra, A. K.; Das, G.; Malonia, S. K. Next-Generation Sequencing Technology: Current Trends and Advancements. *Biology* **2023**, *12* (7). https://doi.org/10.3390/biology12070997.
(46) Supplitt, S.; Karpinski, P.; Sasiadek, M.; Laczmanska, I. Current Achievements and Applications of Transcriptomics in Personalized Cancer Medicine. *International Journal of Molecular Sciences* **2021**, *22* (3), 1422. https://doi.org/10.3390/ijms22031422.
(47) Pasitka, L.; Cohen, M.; Ehrlich, A.; Gildor, B.; Reuveni, E.; Ayyash, M.; Wissotsky, G.; Herscovici, A.; Kaminker, R.; Niv, A.; Bitcover, R.; Dadia, O.; Rudik, A.; Voloschin, A.; Shimoni, M.; Cinnamon, Y.; Nahmias, Y. Spontaneous Immortalization of Chicken Fibroblasts Generates Stable, High-Yield Cell Lines for Serum-Free Production of Cultured Meat. *Nat Food* **2023**, *4* (1), 35–50. https://doi.org/10.1038/s43016-022-00658-w.
(48) Ma, T.; Ren, R.; Yang, R.; Xinyi, Z.; Hu, Y.; Zhu, G.; Wang, H. Transdifferentiation of Fibroblasts into Muscle Cells to Constitute Cultured Meat with Tunable Intramuscular Fat Deposition. *eLife* **2024**, *13*. https://doi.org/10.7554/eLife.93220.1.
(49) Messmer, T.; Klevernic, I.; Furquim, C.; Ovchinnikova, E.; Dogan, A.; Cruz, H.; Post, M. J.; Flack, J. E. A Serum-Free Media Formulation for Cultured Meat Production Supports Bovine Satellite Cell Differentiation in the Absence of Serum Starvation. *Nat Food* **2022**, *3* (1), 74–85. https://doi.org/10.1038/s43016-021-00419-1.
(50) *Measuring RNA with NanoDrop*. Protocol Place. https://protocol-place.com/basic-lab-techniques/rna-purification/measuring-rna-yield-with-a-nanodrop-spectrophotometer/ (accessed 2023-12-22).
(51) Patro, R.; Duggal, G.; Love, M. I.; Irizarry, R. A.; Kingsford, C. Salmon Provides Fast and Bias-Aware Quantification of Transcript Expression. *Nat Methods* **2017**, *14* (4), 417–419. https://doi.org/10.1038/nmeth.4197.
(52) Love, M. I.; Huber, W.; Anders, S. Moderated Estimation of Fold Change and Dispersion for RNA-Seq Data with DESeq2. *Genome Biol* **2014**, *15* (12), 1–21. https://doi.org/10.1186/s13059-014-0550-8.
(53) Stephens, M. False Discovery Rates: A New Deal. *Biostatistics* **2017**, *18* (2), 275–294. https://doi.org/10.1093/biostatistics/kxw041.

(54) Zhu, A.; Ibrahim, J. G.; Love, M. I. Heavy-Tailed Prior Distributions for Sequence Count Data: Removing the Noise and Preserving Large Differences. *Bioinformatics* **2019**, *35* (12), 2084–2092. https://doi.org/10.1093/bioinformatics/bty895.
(55) *Gene set enrichment analysis: A knowledge-based approach for interpreting genome-wide expression profiles | PNAS*. https://www.pnas.org/doi/10.1073/pnas.0506580102 (accessed 2024-04-17).
(56) Tarca, A. L.; Draghici, S.; Khatri, P.; Hassan, S. S.; Mittal, P.; Kim, J.; Kim, C. J.; Kusanovic, J. P.; Romero, R. A Novel Signaling Pathway Impact Analysis. *Bioinformatics* **2009**, *25* (1), 75–82. https://doi.org/10.1093/bioinformatics/btn577.
(57) *org.Bt.eg.db*. Bioconductor. http://bioconductor.org/packages/org.Bt.eg.db/ (accessed 2024-04-17).
(58) Korotkevich, G.; Sukhov, V.; Budin, N.; Shpak, B.; Artyomov, M. N.; Sergushichev, A. Fast Gene Set Enrichment Analysis. bioRxiv February 1, 2021, p 060012. https://doi.org/10.1101/060012.
(59) *Table of Contents*. https://www.gsea-msigdb.org/gsea/doc/GSEAUserGuideTEXT.htm (accessed 2024-05-01).
(60) Chen, J.-Y.; He, X.-X.; Ma, C.; Wu, X.-M.; Wan, X.-L.; Xing, Z.-K.; Pei, Q.-Q.; Dong, X.-P.; Liu, D.-X.; Xiong, W.-C.; Zhu, X.-J. Netrin-1 Promotes Glioma Growth by Activating NF-κB via UNC5A. *Sci Rep* **2017**, *7* (1), 5454. https://doi.org/10.1038/s41598-017-05707-0.
(61) Lee, H. K.; Seo, I. A.; Seo, E.; Seo, S.-Y.; Lee, H. J.; Park, H. T. Netrin-1 Induces Proliferation of Schwann Cells through Unc5b Receptor. *Biochemical and Biophysical Research Communications* **2007**, *362* (4), 1057–1062. https://doi.org/10.1016/j.bbrc.2007.08.143.
(62) Wang, W.; Reeves, W. B.; Ramesh, G. Netrin-1 Increases Proliferation and Migration of Renal Proximal Tubular Epithelial Cells via the UNC5B Receptor. *American Journal of Physiology-Renal Physiology* **2009**, *296* (4), F723–F729. https://doi.org/10.1152/ajprenal.90686.2008.
(63) Kaczynski, P.; Baryla, M.; Goryszewska, E.; Bauersachs, S.; Waclawik, A. Prostaglandin F2α Promotes Embryo Implantation and Development in the Pig. *Reproduction* **2018**, *156* (5), 405–419. https://doi.org/10.1530/REP-18-0225.
(64) Baryla, M.; Kaczynski, P.; Goryszewska, E.; Riley, S. C.; Waclawik, A. Prostaglandin F2α Stimulates Adhesion, Migration, Invasion and Proliferation of the Human Trophoblast Cell Line HTR-8/SVneo. *Placenta* **2019**, *77*, 19–29. https://doi.org/10.1016/j.placenta.2019.01.020.
(65) Fu, C.; Mao, W.; Gao, R.; Deng, Y.; Gao, L.; Wu, J.; Zhang, S.; Shen, Y.; Liu, K.; Li, Q.; Song, X.; Cao, J.; Liu, B. Prostaglandin F2α-PTGFR Signaling Promotes Proliferation of Endometrial Epithelial Cells of Cattle through Cell Cycle Regulation. *Animal Reproduction Science* **2020**, *213*, 106276. https://doi.org/10.1016/j.anireprosci.2020.106276.
(66) Miao, J.; Ding, M.; Zhang, A.; Xiao, Z.; Qi, W.; Luo, N.; Di, W.; Tao, Y.; Fang, Y. Pleiotrophin Promotes Microglia Proliferation and Secretion of Neurotrophic Factors by Activating Extracellular Signal-Regulated Kinase 1/2 Pathway. *Neuroscience Research* **2012**, *74* (3), 269–276. https://doi.org/10.1016/j.neures.2012.09.001.
(67) Soh, B. S.; Song, C. M.; Vallier, L.; Li, P.; Choong, C.; Yeo, B. H.; Lim, E. H.; Pedersen, R. A.; Yang, H. H.; Rao, M.; Lim, B. Pleiotrophin Enhances Clonal Growth and Long-Term Expansion

of Human Embryonic Stem Cells. *STEM CELLS* **2007**, *25* (12), 3029–3037. https://doi.org/10.1634/stemcells.2007-0372.

(68) Furue, M. K.; Na, J.; Jackson, J. P.; Okamoto, T.; Jones, M.; Baker, D.; Hata, R.-I.; Moore, H. D.; Sato, J. D.; Andrews, P. W. Heparin Promotes the Growth of Human Embryonic Stem Cells in a Defined Serum-Free Medium. *Proc Natl Acad Sci U S A* **2008**, *105* (36), 13409–13414. https://doi.org/10.1073/pnas.0806136105.

(69) Ling, L.; Camilleri, E. T.; Helledie, T.; Samsonraj, R. M.; Titmarsh, D. M.; Chua, R. J.; Dreesen, O.; Dombrowski, C.; Rider, D. A.; Galindo, M.; Lee, I.; Hong, W.; Hui, J. H.; Nurcombe, V.; van Wijnen, A. J.; Cool, S. M. Effect of Heparin on the Biological Properties and Molecular Signature of Human Mesenchymal Stem Cells. *Gene* **2016**, *576* (1 Pt 2), 292–303. https://doi.org/10.1016/j.gene.2015.10.039.

(70) Ting, H.-A.; Schaller, M. A.; de Almeida Nagata, D. E.; Rasky, A. J.; Maillard, I. P.; Lukacs, N. W. Notch Ligand Delta-like 4 Promotes Regulatory T Cell Identity in Pulmonary Viral Infection. *The Journal of Immunology* **2017**, *198* (4), 1492–1502. https://doi.org/10.4049/jimmunol.1601654.

(71) Awad, K.; Wang, S.; Dougherty, E.; Keshavarz, A.; Curran, C.; Miller, L.; Elinoff, J. M.; Danner, R. L. DLL4/NOTCH1 Induces PPPARγ, Suppressing AKT and the Proliferative, Apoptosis Resistant Phenotype of BMPR2-Silenced Pulmonary Artery Endothelial Cells. In *C26. UNRAVELING THE GORDIAN KNOT: MULTI-DIMENSIONAL -OMICs AND SIGNALING MOTIFS IN PULMONARY VASCULAR DISEASE*; American Thoracic Society, 2023; pp A4662–A4662. https://doi.org/10.1164/ajrccm-conference.2023.207.1_MeetingAbstracts.A4662.

(72) Xu, C.; Wu, X.; Zhu, J. VEGF Promotes Proliferation of Human Glioblastoma Multiforme Stem-Like Cells through VEGF Receptor 2. *The Scientific World Journal* **2013**, *2013*, e417413. https://doi.org/10.1155/2013/417413.

(73) Coppola, S.; Narciso, L.; Feccia, T.; Bonci, D.; Calabrò, L.; Morsilli, O.; Gabbianelli, M.; De Maria, R.; Testa, U.; Peschle, C. Enforced Expression of KDR Receptor Promotes Proliferation, Survival and Megakaryocytic Differentiation of TF1 Progenitor Cell Line. *Cell Death Differ* **2006**, *13* (1), 61–74. https://doi.org/10.1038/sj.cdd.4401698.

(74) Li, W.; Lu, Z.-F.; Man, X.-Y.; Li, C.-M.; Zhou, J.; Chen, J.-Q.; Yang, X.-H.; Wu, X.-J.; Cai, S.-Q.; Zheng, M. VEGF Upregulates VEGF Receptor-2 on Human Outer Root Sheath Cells and Stimulates Proliferation through ERK Pathway. *Mol Biol Rep* **2012**, *39* (9), 8687–8694. https://doi.org/10.1007/s11033-012-1725-6.

(75) Calise, S.; Blescia, S.; Cencetti, F.; Bernacchioni, C.; Donati, C.; Bruni, P. Sphingosine 1-Phosphate Stimulates Proliferation and Migration of Satellite Cells: Role of S1P Receptors. *Biochimica et Biophysica Acta (BBA) - Molecular Cell Research* **2012**, *1823* (2), 439–450. https://doi.org/10.1016/j.bbamcr.2011.11.016.

(76) Cheng, J.-C.; Wang, E. Y.; Yi, Y.; Thakur, A.; Tsai, S.-H.; Hoodless, P. A. S1P Stimulates Proliferation by Upregulating CTGF Expression through S1PR2-Mediated YAP Activation. *Molecular Cancer Research* **2018**, *16* (10), 1543–1555. https://doi.org/10.1158/1541-7786.MCR-17-0681.

(77) Wang, J.; Yan, X.; Feng, W.; Wang, Q.; Shi, W.; Chai, L.; Zhang, Q.; Chen, Y.; Liu, J.; Qu, Z.; Xie, X.; Li, M. S1P Induces Proliferation of Pulmonary Artery Smooth Muscle Cells by Promoting YAP-Induced Notch3 Expression and Activation. *J Biol Chem* **2021**, *296*, 100599. https://doi.org/10.1016/j.jbc.2021.100599.

(78) Yoshioka, H.; Ramakrishnan, S. S.; Shim, J.; Suzuki, A.; Iwata, J. Excessive All-Trans Retinoic Acid Inhibits Cell Proliferation Through Upregulated MicroRNA-4680-3p in Cultured Human Palate Cells. *Frontiers in Cell and Developmental Biology* **2021**, *9*.
(79) De Angelis, M. T.; Parrotta, E. I.; Santamaria, G.; Cuda, G. Short-Term Retinoic Acid Treatment Sustains Pluripotency and Suppresses Differentiation of Human Induced Pluripotent Stem Cells. *Cell Death Dis* **2018**, *9* (1), 1–13. https://doi.org/10.1038/s41419-017-0028-1.
(80) Zhao, L.; Son, J. S.; Wang, B.; Tian, Q.; Chen, Y.; Liu, X.; de Avila, J. M.; Zhu, M.-J.; Du, M. Retinoic Acid Signalling in Fibro/Adipogenic Progenitors Robustly Enhances Muscle Regeneration. *EBioMedicine* **2020**, *60*, 103020. https://doi.org/10.1016/j.ebiom.2020.103020.
(81) Neuville, P.; Yan, Z. -q; Gidlöf, A.; Pepper, M. S.; Hansson, G. K.; Gabbiani, G.; Sirsjö, A. Retinoic Acid Regulates Arterial Smooth Muscle Cell Proliferation and Phenotypic Features In Vivo and In Vitro Through an RARα-Dependent Signaling Pathway. *Arteriosclerosis, Thrombosis, and Vascular Biology* **1999**, *19* (6), 1430–1436. https://doi.org/10.1161/01.ATV.19.6.1430.
(82) Bai, F.; Yang, G.; Eskew, J.; Wang, N.; Bose, H.; Zhao, Z. Antagonism of Angiotensin II AT1 Receptor and Silencing of CD44 Gene Expression Inhibit Cardiac Fibroblast Activation via Modulating TGF- β 1/Smad Signaling Pathway. *Advances in Bioscience and Biotechnology* **2020**, *11*, 123–139. https://doi.org/10.4236/abb.2020.114010.
(83) Chao, J.; Yang, L.; Buch, S.; Gao, L. Angiotensin II Increased Neuronal Stem Cell Proliferation: Role of AT2R. *PLOS ONE* **2013**, *8* (5), e63488. https://doi.org/10.1371/journal.pone.0063488.
(84) Zhang, F.; Ren, X.; Zhao, M.; Zhou, B.; Han, Y. Angiotensin-(1–7) Abrogates Angiotensin II-Induced Proliferation, Migration and Inflammation in VSMCs through Inactivation of ROS-Mediated PI3K/Akt and MAPK/ERK Signaling Pathways. *Sci Rep* **2016**, *6*, 34621. https://doi.org/10.1038/srep34621.
(85) Yang, X.; Zhu, M. J.; Sreejayan, N.; Ren, J.; Du, M. Angiotensin II Promotes Smooth Muscle Cell Proliferation and Migration through Release of Heparin-Binding Epidermal Growth Factor and Activation of EGF-Receptor Pathway. *Molecules and Cells* **2005**, *20* (2), 263–270. https://doi.org/10.1016/S1016-8478(23)13226-2.
(86) Yuan, L.; Sheng, X.; Willson, A. K.; Roque, D. R.; Stine, J. E.; Guo, H.; Jones, H. M.; Zhou, C.; Bae-Jump, V. L. Glutamine Promotes Ovarian Cancer Cell Proliferation through the mTOR/S6 Pathway. *Endocrine-Related Cancer* **2015**, *22* (4), 577–591. https://doi.org/10.1530/ERC-15-0192.
(87) Cacace, A.; Sboarina, M.; Vazeille, T.; Sonveaux, P. Glutamine Activates STAT3 to Control Cancer Cell Proliferation Independently of Glutamine Metabolism. *Oncogene* **2017**, *36* (15), 2074–2084. https://doi.org/10.1038/onc.2016.364.
(88) Sheng, H.; Shao, J.; Washington, M. K.; DuBois, R. N. Prostaglandin E2 Increases Growth and Motility of Colorectal Carcinoma Cells*. *Journal of Biological Chemistry* **2001**, *276* (21), 18075–18081. https://doi.org/10.1074/jbc.M009689200.
(89) Mo, C.; Zhao, R.; Vallejo, J.; Igwe, O.; Bonewald, L.; Wetmore, L.; Brotto, M. Prostaglandin E2 Promotes Proliferation of Skeletal Muscle Myoblasts via EP4 Receptor Activation. *Cell Cycle* **2015**, *14* (10), 1507–1516. https://doi.org/10.1080/15384101.2015.1026520.

(90) Li, N.; Yan, Y.-L.; Fu, S.; Li, R.-J.; Zhao, P.-F.; Xu, X.-Y.; Yang, J.-P.; Damirin, A. Lysophosphatidic Acid Enhances Human Umbilical Cord Mesenchymal Stem Cell Viability without Differentiation via LPA Receptor Mediating Manner. *Apoptosis* **2017**, *22* (10), 1296–1309. https://doi.org/10.1007/s10495-017-1399-6.

(91) Leve, F.; Peres-Moreira, R. J.; Binato, R.; Abdelhay, E.; Morgado-Díaz, J. A. LPA Induces Colon Cancer Cell Proliferation through a Cooperation between the ROCK and STAT-3 Pathways. *PLoS One* **2015**, *10* (9), e0139094. https://doi.org/10.1371/journal.pone.0139094.

(92) Oshi, M.; Patel, A.; Le, L.; Tokumaru, Y.; Yan, L.; Matsuyama, R.; Endo, I.; Takabe, K. G2M Checkpoint Pathway Alone Is Associated with Drug Response and Survival among Cell Proliferation-Related Pathways in Pancreatic Cancer. *Am J Cancer Res* **2021**, *11* (6), 3070–3084.

(93) Zhang, Y.; Alexander, P. B.; Wang, X.-F. TGF-β Family Signaling in the Control of Cell Proliferation and Survival. *Cold Spring Harb Perspect Biol* **2017**, *9* (4), a022145. https://doi.org/10.1101/cshperspect.a022145.

(94) Abid, Md. R.; Guo, S.; Minami, T.; Spokes, K. C.; Ueki, K.; Skurk, C.; Walsh, K.; Aird, W. C. Vascular Endothelial Growth Factor Activates PI3K/Akt/Forkhead Signaling in Endothelial Cells. *Arteriosclerosis, Thrombosis, and Vascular Biology* **2004**, *24* (2), 294–300. https://doi.org/10.1161/01.ATV.0000110502.10593.06.

(95) Mebratu, Y.; Tesfaigzi, Y. How ERK1/2 Activation Controls Cell Proliferation and Cell Death Is Subcellular Localization the Answer? *Cell Cycle* **2009**, *8* (8), 1168–1175.

(96) Sun, Y.; Liu, W.-Z.; Liu, T.; Feng, X.; Yang, N.; Zhou, H.-F. Signaling Pathway of MAPK/ERK in Cell Proliferation, Differentiation, Migration, Senescence and Apoptosis. *Journal of Receptors and Signal Transduction* **2015**, *35* (6), 600–604. https://doi.org/10.3109/10799893.2015.1030412.

(97) *L-Glutamine and GlutaMAX Supplement - US*. https://www.thermofisher.com/us/en/home/life-science/cell-culture/mammalian-cell-culture/media-supplements/glutamax-media.html (accessed 2024-04-17).

(98) Weddell, J. C.; Chen, S.; Imoukhuede, P. I. VEGFR1 Promotes Cell Migration and Proliferation through PLCγ and PI3K Pathways. *npj Syst Biol Appl* **2017**, *4* (1), 1–11. https://doi.org/10.1038/s41540-017-0037-9.

(99) An, S.; Zheng, Y.; Bleu, T. Sphingosine 1-Phosphate-Induced Cell Proliferation, Survival, and Related Signaling Events Mediated by G Protein-Coupled Receptors Edg3 and Edg5 *. *Journal of Biological Chemistry* **2000**, *275* (1), 288–296. https://doi.org/10.1074/jbc.275.1.288.

(100) *CyQUANT™ Cell Proliferation Assay, for cells in culture*. https://www.thermofisher.com/order/catalog/product/C7026 (accessed 2024-04-17).

(101) Lundholt, B. K.; Scudder, K. M.; Pagliaro, L. A Simple Technique for Reducing Edge Effect in Cell-Based Assays. *J Biomol Screen* **2003**, *8* (5), 566–570. https://doi.org/10.1177/1087057103256465.

(102) Romero, S. G.; Boyle, N. Systems Biology and Metabolic Modeling for Cultivated Meat: A Promising Approach for Cell Culture Media Optimization and Cost Reduction. *Comprehensive Reviews in Food Science and Food Safety* **2023**, *22* (4), 3422–3443. https://doi.org/10.1111/1541-4337.13193.

(103) Stout, A. J.; Zhang, X.; Letcher, S. M.; Rittenberg, M. L.; Shub, M.; Chai, K. M.; Kaul, M.; Kaplan, D. L. Engineered Autocrine Signaling Eliminates Muscle Cell FGF2 Requirements for Cultured Meat Production. *bioRxiv* **2023**, 2023.04.17.537163. https://doi.org/10.1101/2023.04.17.537163.

Chapter 7. Supplementary Tables and Figures

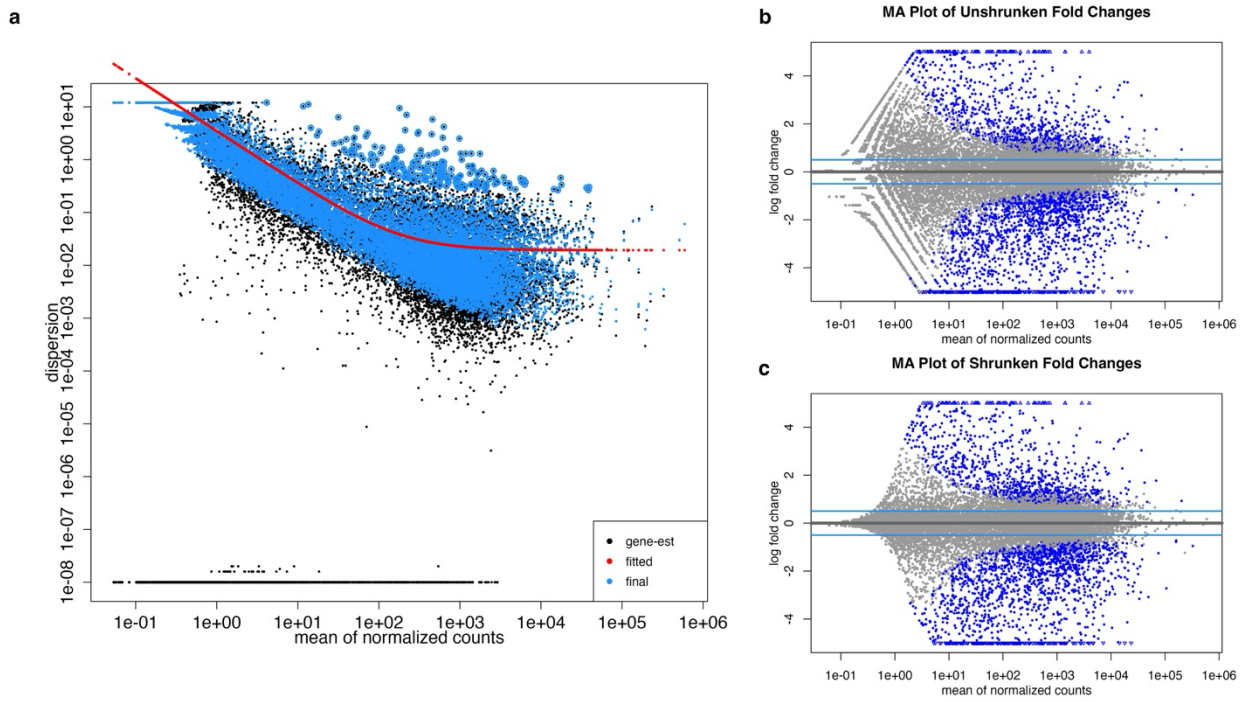

Supp. Figure 1. Gene-wise dispersion and shrinkage. (a) Plot of estimated gene dispersion vs. mean of normalized counts, fitted model, and final dispersion estimates. (b), (c) MA plot (log2FC vs. mean of normalized counts) for unshrunk and shrunken fold changes.

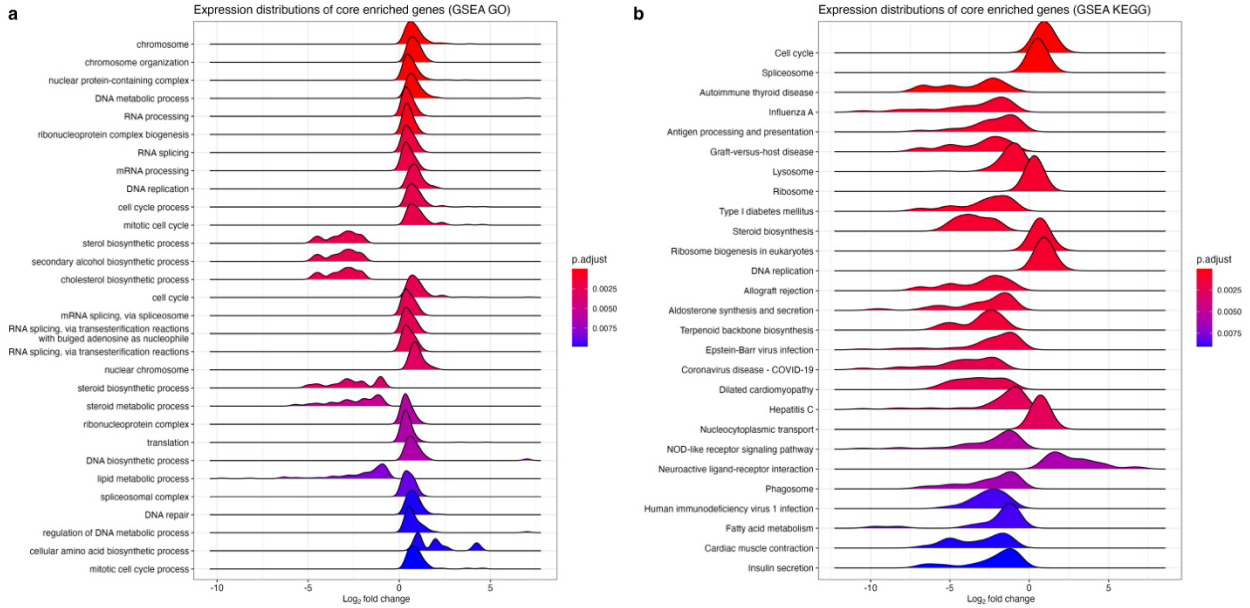

Supp. Figure 2. Expression distributions based on log2FC of significantly observed GO and KEGG pathways. (a) Distributions of GO terms. (b) Distributions of KEGG terms.

Sample	Concentration (ng/ul)	A260/A280	A260/A230
GM-1	382.4	2	1.77
GM-2	287.3	2.06	1.92
GM-3	345.8	2.08	1.74
GM-4	233.2	2.02	1.32
BR-1	254.2	2.07	1.96
BR-2	605.8	2.04	1.57
BR-3	280	2.06	1.94
BR-4	264.8	2.08	1.83
B9-1	376.3	2.07	1.13
B9-2	287.8	2.07	1.98
B9-3	479	2.03	1.83
B9-4	215.2	2.06	1.75

Supp. Table 1. RNA nanodrop data for all samples showing quality of RNA.

Receptor	Log2FC	Adjusted p-value	Rank
GPR68	9.185	7.793E-144	3077
UNC5B	6.616	2.251E-98	1521
RARB	7.970	5.040E-62	1160
PTGFR	6.547	1.188E-74	1144
MEG8	10.26	2.895E-41	998.9
ALK	5.410	3.555E-60	764.5
GRIA3	3.291	9.533E-80	614.2
PPARG	8.572	1.054E-27	563.9
CRLF1	6.559	4.497E-35	544.2
RARRES1	5.252	2.149E-39	488.6
NOTCH1	2.068	4.495E-83	402.0
LOC100298064	4.320	1.707E-36	372.7
KDR	5.522	7.003E-17	223.2
LOC101905194	6.358	5.920E-14	213.3
LIFR	4.756	5.866E-14	159.6
FLT1	5.969	1.018E-10	154.6
GREB1L	3.060	1.728E-19	142.4
AGTR1	3.867	1.086E-13	127.2
GPR63	4.685	3.369E-11	126.7
LOC101906312	4.680	1.816E-10	118.3
DCC	4.642	1.816E-10	117.4
LOC101905257	5.102	4.534E-09	111.9
SPSB4	4.026	1.982E-11	111.1
MINAR1	5.119	2.975E-08	102.4

Supp. Table 2. Top 25 receptors upregulated in BSC-GM ordered by rank metric.

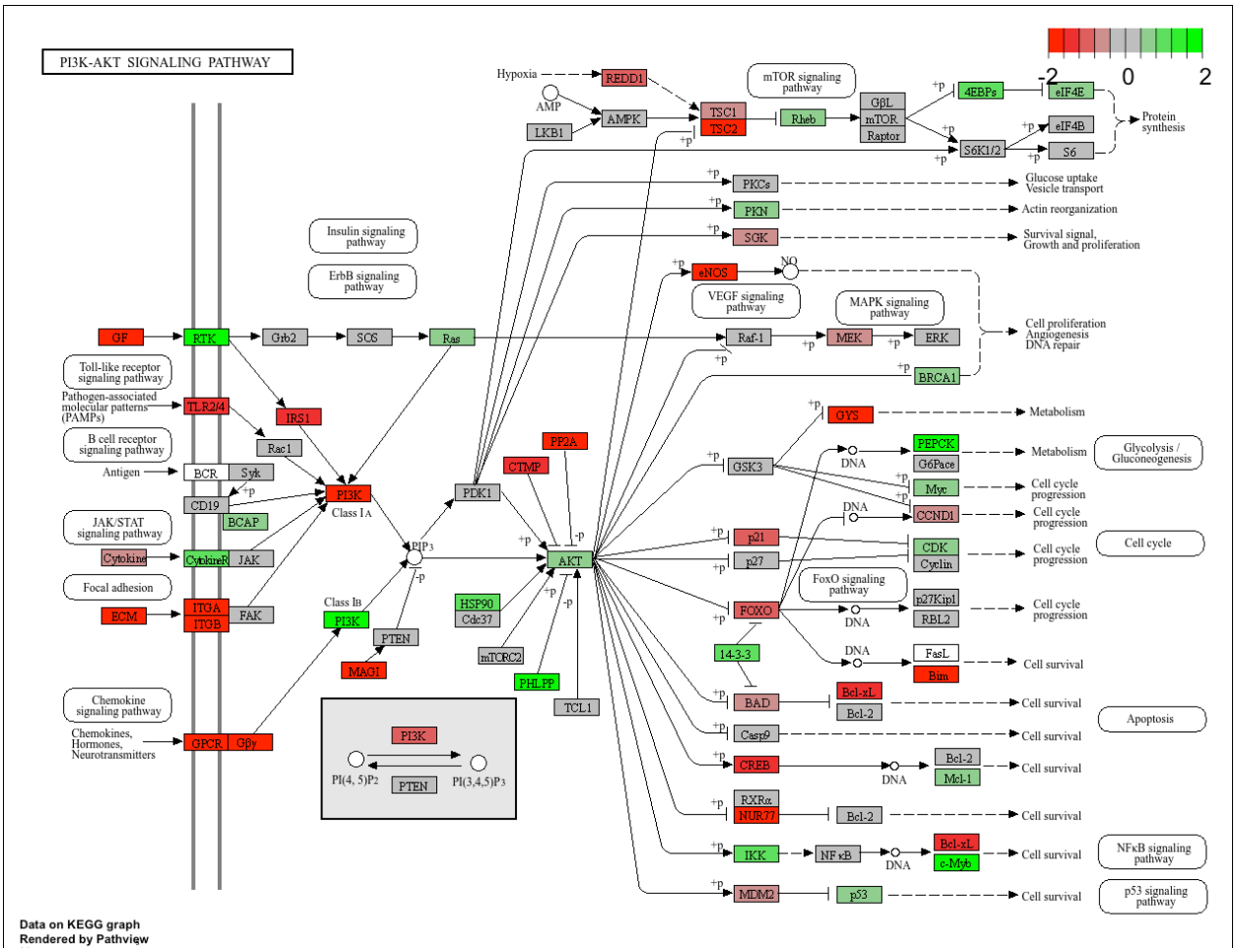

Supp. Figure 3. Genes from RNA seq differentially expressed between BSC-GM and SFM in PI3K-Akt signaling pathway; color corresponds to relative up- or downregulation on a scale from [-2, 2].